



# Magnetostratigraphic dating of earliest hominin sites in Europe

Luis Gibert<sup>a,\*</sup>, Gary Scott<sup>b</sup>, Alan Deino<sup>b</sup>, Robert Martin<sup>c</sup>

<sup>a</sup> Faculty of Earth Sciences, University of Barcelona, Spain

<sup>b</sup> Berkeley Geochronology Center, USA

<sup>c</sup> Murray State University, USA

## ARTICLE INFO

### Keywords:

Magnetostratigraphy  
Olduvai  
Jaramillo  
Early hominins  
Orce  
Oldowan  
Dispersion routes

## ABSTRACT

After a century of research, the chronology of the first arrival of hominins in Europe remains controversial. Four Spanish localities potentially record evidence of the oldest Europeans, yet arrival ages remain loosely constrained between 1.6 and 0.9 Ma. Here we provide a new Early Pleistocene magnetostratigraphy, recording four paleomagnetic boundaries within 80 m of a fluvio-lacustrine sedimentary succession in Orce, southeastern Spain. This Pleistocene succession incorporates for the first time in Europe five superposed paleontological localities between the Olduvai and Jaramillo magnetozones, including three hominin sites providing evidence of the presence of hominins older than 1.07 Ma in Europe. The specific age for each fossil quarry is estimated using a Bayesian age-stratigraphic model with 95% confidence intervals. The oldest sites, which lack evidence of hominin activity, are  $1.60 \pm 0.05$  Ma and  $1.35 \pm 0.07$  Ma, respectively. Three sites higher in the stratigraphy, which contain evidence of hominids, occur at  $1.32 \pm 0.07$  Ma (Venta Micena),  $1.28 \pm 0.07$  Ma (Barranco León-5), and  $1.23 \pm 0.06$  Ma (Fuente Nueva-3). The magnetostratigraphy and paleontological content of the Orce hominin sites are compared with other European localities concluding that the new chronology for Orce represents Europe's oldest and most accurately dated early Pleistocene hominin records. These results indicate that African hominins with Oldowan technology reached Southwestern Europe  $>0.5$  Ma after first leaving Africa. This diachronism is explained because Europe was limited by biogeographical barriers that hominins were able to surpass only in a later evolutionary/cultural stage. We propose that  $\sim 1.3$  Ma hominins first arrived in southern Europe by traversing the Strait of Gibraltar when in a similar time frame, crossed the Wallace Line and reached the island of Flores (Java) by navigating the wider Lombok Strait. Archaeological data shows that a second wave of hominins with Acheulian technology entered South Europe again via the Iberian Peninsula after the Jaramillo subchron (1.071–0.991 Ma) and before the Brunhes chron (0.77 Ma).

## 1. Introduction

### 1.1. Background of evolving European chronologies and present debate

The chronology of *Homo* dispersal out of Africa has expanded significantly in the past four decades. In 1982, the oldest evidence of *Homo* in Asia was paleomagnetically dated at 0.9 Ma in Java, and at 0.7 Ma in Europe in Italy (Pope, 1983; Coltorti et al., 1982). Forty years later, the chronology of early *Homo* beyond Africa was extended to 1.8 Ma in the southern Caucasus (Gabunia et al., 2000; Ferring et al., 2011), 1.7–2.1 Ma in China (Zhu et al., 2008, 2018), and  $> 1.5$  to 1.3 Ma in Java (Larick et al., 2001; Matsu'ura et al., 2020). In Europe, some sites occur in strata with meters of reversed paleomagnetic polarity, indicating they are older than 0.77 Ma, which corresponds to the Brunhes-Matuyama

paleomagnetic boundary (Simon et al., 2018; Channell et al., 2020). However, a more precise assessment of their age has proven difficult due to the absence of volcanic materials for radiometric dating, limited magnetostratigraphic studies, the absence of precise mammalian biostratigraphy, and large errors in alternative dating techniques. This uncertainty has permitted a protracted debate regarding the timing of the earliest occupation, with opinions that support an early arrival ( $>1.3$  Ma) (Carbonell et al., 2008; Scott et al., 2007; Toro-Moyano et al., 2013), while others conclude that hominins arrived in Europe after the Jaramillo event ( $<1$  Ma) (Muttoni et al., 2010, 2015, 2018; Muttoni and Kent, 2024). Human presence at the gates of Europe is recognized at 1.8 Ma south of the Caucasus Mountains (41°N latitude) and at  $>2$  Ma in North Africa (36°N) (Gabunia et al., 2000; Ferring et al., 2011; Sahnouni et al., 2018). The only sites in Europe that exhibit associated *Homo* sp.,

\* Corresponding author.

E-mail address: [lgibert@ub.edu](mailto:lgibert@ub.edu) (L. Gibert).

<https://doi.org/10.1016/j.earscirev.2024.104855>

Received 12 January 2024; Received in revised form 17 June 2024; Accepted 28 June 2024

Available online 2 July 2024

0012-8252/© 2024 The Authors. Published by Elsevier B.V. This is an open access article under the CC BY-NC-ND license (<http://creativecommons.org/licenses/by-nc-nd/4.0/>).

Oldowan tools, and vertebrate fauna potentially older than 1 Ma occur in north-central Spain at the karstic site of Sima del Elefante (42°N), and in southeastern Spain in the lacustrine deposits of Orce (37°N) (Carbonell et al., 2008, Scott et al., 2007, Toro-Moyano et al., 2013), (Fig. 1).

### 1.2. The Orce sites

The Orce region occurs in the NE sector of the large (>1000km<sup>2</sup>) intramountain Baza Basin in the Betic range (SE Spain), (SI). This area exposes >50 km<sup>2</sup> of Early Pleistocene sedimentary strata rich in vertebrate fossils (Fig. 2, SI). Field surveys in 1976 and 1979 led by the late Dr. Josep Gibert, produced the discovery of several fossiliferous strata in this region (Gibert, 2008). Initial excavations in 1982 at the extensive lacustrine Venta Micena site (>10<sup>6</sup>m<sup>2</sup>) uncovered a skull fragment at quarry-3 attributed to an infant *Homo* sp. (named VM-0), associated with an abundant early Pleistocene fauna with an estimated age of >1 Ma. This association evinced a much older age than previously believed for *Homo* in Europe and Asia (Gibert et al., 1983). VM-0 consists of two parietal bones and part of the occipital bone with a 4 mm endocranial crest (SI). This anatomy initially led some critics to question an affinity with *Homo* attributing alternatively this fossil to a young horse (Agustí and Moyà-Solà, 1987; Moyà-Solà and Köhler, 1997) or a ruminant (Martínez-Navarro, 2002) without being able to reproduce the VM-

0 anatomy in those mammals. In contrast, descriptions of similar endocranial crests in infant human skulls together with other anatomical traits, have permitted to replicate the anatomy of VM-0 skull in the *homo* genus (Campillo, 1989; Campillo et al., 2006; Gibert et al., 1989a, b, Gibert et al., 1998a, b). In addition, the identification of two human humeral shafts (VM-1960, VM-3691) (Sánchez et al., 1999) and recovery of a limited archaeological assemblage, and a record of stone-tool processing of animal tissues, further supported the presence of *Homo* at quarry VM-3 of Venta Micena (Gibert and Ferrández, 1989, Gibert and Martínez-Navarro, 1992, Gibert and Jiménez, 1991, Gibert et al., 1992a, 1992b, 1994, 2006a, 2006b, SI). Subsequent anatomical (Campillo et al., 2006; Gibert et al., 1998a) and conclusive paleoproteomic studies (Borja et al., 1997; Lowenstein et al., 1999; Torres et al., 2022) have strongly supported the attribution of these three fossils to *Homo* (Aguirre, 2008). “To summarise on the contribution which Venta Micena has made to our thinking on early hominids in Europe, from that site specifically, the identification - by anatomical and molecular means of hominid bones provides critical evidence that hominids were present at Venta Micena in the Early Pleistocene.” (Tobias, 1998).

Excavations at Venta Micena quarry-3 were discontinuous between 1982 and 1995, and no extensive excavations have been developed since. In 2014, investigations at Venta Micena were resumed 360 m south of the hominin VM-3 quarry, at VM-8 quarry where human

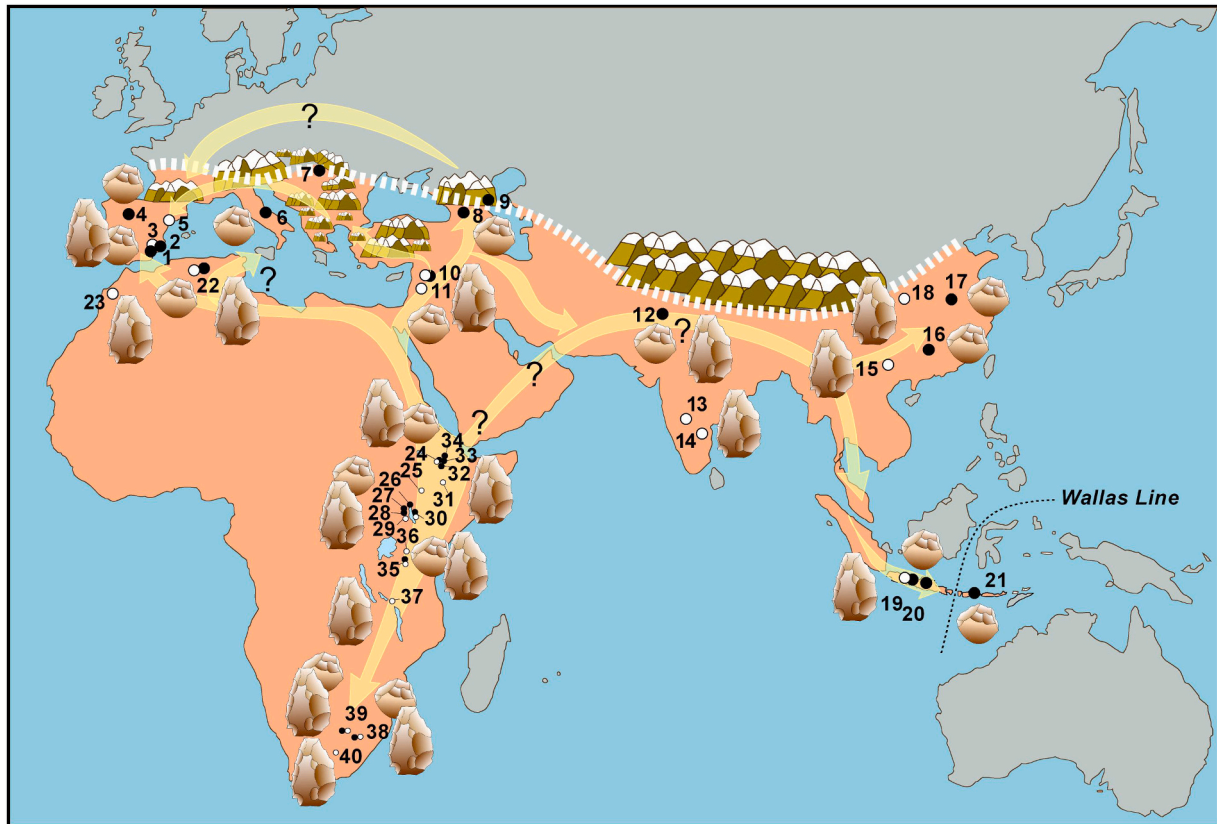


**Fig. 1.** Key dated sites showing the world distribution of hominins before 1 Ma (orange colour) and potential dispersion routes (more European sites in Fig. 11). The figure shows sites with Oldowan technology (black dots) older than 2 Ma in Africa and close or older than 1 Ma in Eurasia. White dots show the oldest Acheulian sites in Africa (>1.5 Ma) and in Eurasia (between 1 and 0.8 Ma). The oldest Oldowan and Acheulian tools occur in East Africa at >2.5 Ma (28, 24,34) and > 1.7 Ma (25, 29,35) respectively. In Asia, the oldest Oldowan and Acheulian occur in the Caucasus at 1.8 Ma (8) and in the Levant corridor at 1.2 Ma (10) respectively. In Europe the oldest Oldowan and associated hominins occur in Spain (1) with a debated age 1.6–0.9 Ma (Muttoni et al., 2010, 2015; Carbonell et al., 2008; Toro-Moyano et al., 2013; Scott et al., 2007). The oldest European Acheulian occurs also in Spain between 0.99 Ma and 0.77 Ma (3, 5, Scott and Gibert, 2009, Vallverdú et al., 2014). **Europe:** 1. Orce, 2. Cueva Victoria, 3 Cueva Negra, 4. Atapuerca, 5. Barranc de la Boella, 6 Pirro Nord, 7 Korolevo. **West Asia:** 8. Dmanisi, 9 Muhkai-2, 10. Ubeidiya, 11. Geshen Benot. **Central Asia:** 12. Riwayat, 13. Isampur, 14 Attirampakkam. **East Asia:** 15. Bose, 16. Yuanmou Basin, 17. Nihewan Basin, 18. Lounan Basin, 19 Sangiran, 20. Mojokerto, 21. Flores. **Africa:** 22. Ain Hanech, Ain Ain Boucherit 23. Thomas-1, 24. Gona, 25. Konso Kandula, 26. Omo, 27. Lokalalei, 28 Lomekwi, 29 Kokiselei 30, Kobi Fora, 31 Gaded, 32 M. Awash, 33 Hadar, 34 Ledi Geraru, 35 Olduvai, 36 Peninj, 37 Mwanganda, 38. Sterkfontein, 39 Swartkrans, 40 Vaal River, (Harmand et al., 2015, Zhu et al., 2008, Simanjuntak et al., 2010, Lepre et al., 2011, Diez-Martín et al., 2015, Belmaker et al., 2002, David R. Braun et al., 2019, Sahnouni et al., 2018, Pappu et al., 2011, Trifonov et al., 2019) and references within. See Fig. 11 for more details in Europe.

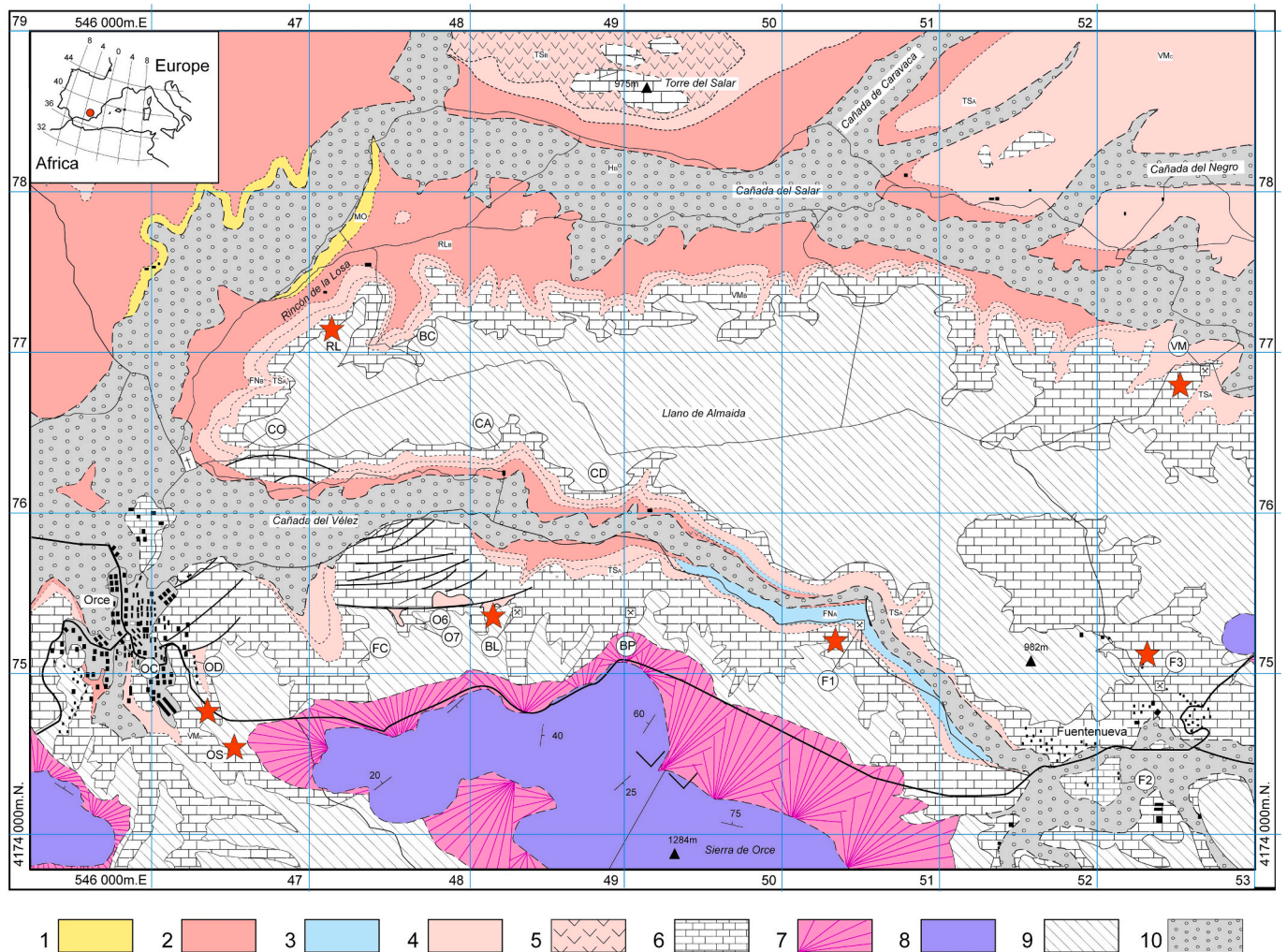


**Fig. 2.** New geological map of the study area with location of paleontological localities and studied sections (red stars). Sites: OC=Orce C; OD=Orce D; FC = Fuentecica; O6 = Orce 6; O7 = Orce 7; BL = Barranco León; BP=Barranco del Paso; F1 = Fuente Nueva 1; F2 = Fuente Nueva 2; F3 = Fuente Nueva 3; CD=Cortijo Don Diego; CA = Cortijo Don Alfonso; CO=Cementerio Orce; BC = Barranco de los Conejos; VM = Venta Micena. The squares in the map are 1 km<sup>2</sup>. Legend 1: Molino lacustrine limestones (Mo), 2 Rincón de la Losa reddish siltstones (RLa), 3 Fuente Nueva lacustrine limestones with chert (FNa), 4 Torre del Salar (TSA) and Fuente Nueva siltstones (FNb), 5 Torre del Salar siltstones with gypsum (TSb), 6 Venta Micena palustrine limestones (VMb), 7 colluvial deposits (Ps), 8 Jurassic limestones, 9 Erosional surface 10 Holocene valley infill (Hb), (see SI for expanded map and legend). (For interpretation of the references to colour in this figure legend, the reader is referred to the web version of this article.)

presence has never been identified (Gibert et al., 2003b, Luzón et al., 2021, Yravedra et al., 2023, SI). However, the discovery of two deciduous human molars (Gibert et al., 1999; Toro-Moyano et al., 2013; Ribot et al., 2015) and thousands of Oldowan lithic tools and cut marks on bones at the nearby sites of Barranco León-5 (BL-5) and Fuente Nueva-3 (FN-3) (Gibert et al., 1992, 1998a, 1998b; Toro-Moyano et al., 2013; Tittton et al., 2020; Yravedra et al., 2021, 2022) solidified evidence for the presence of *Homo* in the Early Pleistocene of Orce, shifting the focus of the debate to site chronology (Muttoni et al., 2010, 2015). The three hominin sites occur within a relatively short period in the same lithostratigraphic unit, associated with a similar faunal assemblage (Fig. 2, Fig. 3, SI).

### 1.3. Evolving chronology of the Orce sites

Faunal assemblages of the Orce sites were initially dated as Early Pleistocene based on biostratigraphy (Gibert et al., 1983). The lack of volcanic material for radiometric dating in the Baza basin leaves paleomagnetism as an alternative technique to refine the age of the archaeological sites. An initial magnetostratigraphic study identified 35 m of reverse polarity at FN-1 section and placed this section between

0.77 Ma and 2.58 Ma (Oms et al., 1996). A second study claimed to identify the Olduvai subchron in the upper 10 m of the Barranco de Orce section (Agustí et al., 1997). The lower boundary of the Olduvai subchron was placed at a similar stratigraphic level as the BL-5 site which is located 300 m to the east, suggesting an age of >1.93 Ma for BL-5 fossil/tools material (Gibert et al., 1998b). A review of this magnetostratigraphy proved that the rocks from Barranco de Orce were remagnetized in the present field direction, invalidating older chronologies (Gibert et al., 2006a). After the international conference held in Orce in 1995 (Zihlman and Lowenstein, 1996), Dr. J. Gibert invited Dr. J.M Parés to sample the recently opened Barranco León quarry, but according to Parés, the paleomagnetic results were ambiguous (Gibert, 2006). Posterior studies at the same quarry and also at the Fuente Nueva-3 section done by Parés and others showed only reverse polarity, dating the sites to older than the Brunhes/Matuyama boundary (0.77 Ma), (Oms et al., 2000; Gibert et al., 2006a, 2006b). In 2007, a more extensive study incorporating 60 m of the Orce stratigraphy demonstrated a polarity sequence of three magnetozones with a sequence of reverse-normal-reverse polarity. Various field tests were performed to demonstrate that the normal zone was not remagnetized (Scott et al., 2007). Paleontological data permitted correlation of the normal zone

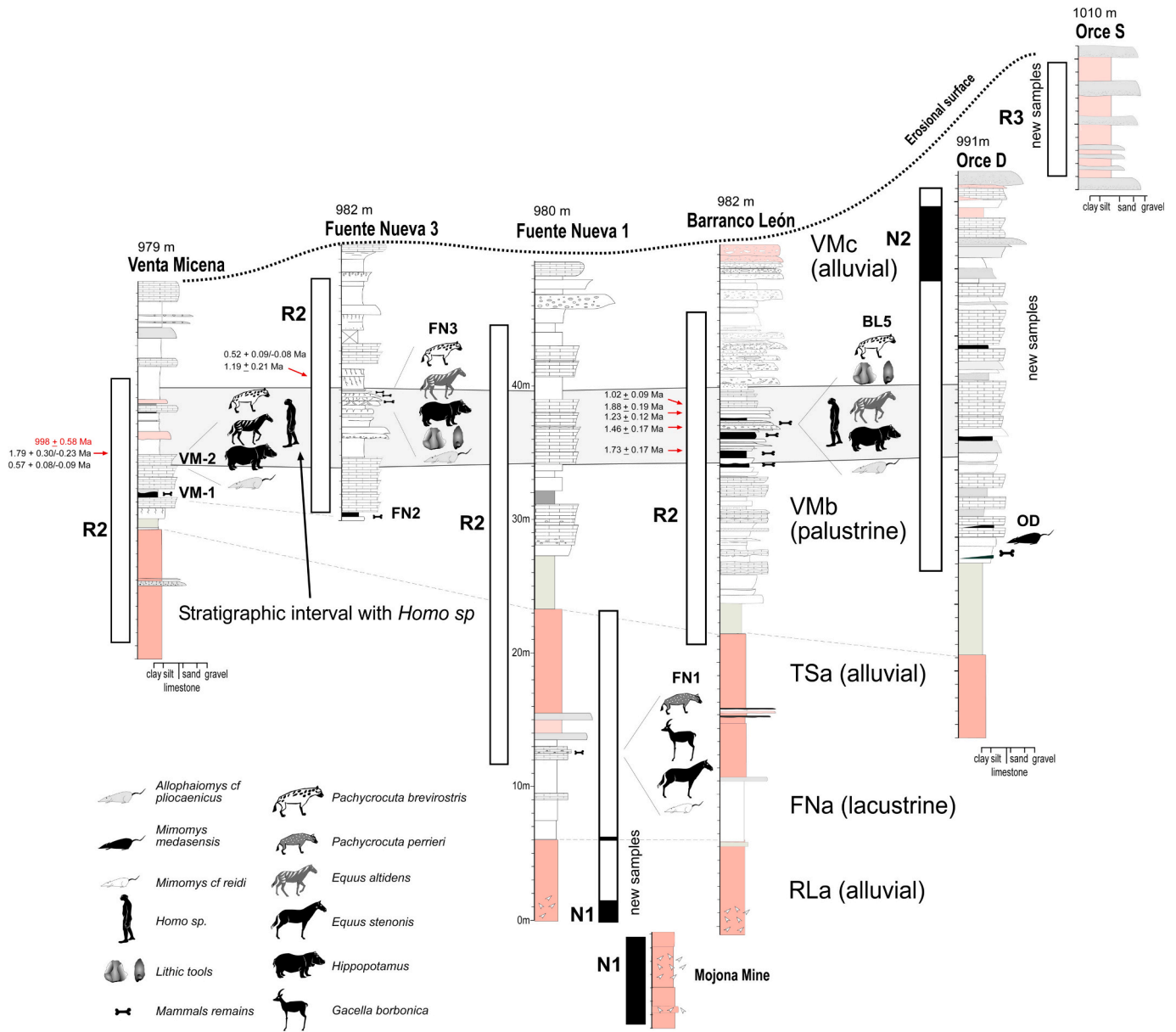


**Fig. 3.** Below: stratigraphic correlation with a summary of new and published paleomagnetic results along the Salar Valley (FN-3 to OD) and Venta Micena section in the Vélez Valley. The figure shows the location of hominin sites in an approximate 6 m thick stratigraphic interval of reversed polarity between N1 and N2 associated with *Allophaiomys cf. plicicaenicus*. The figure shows the last appearance datum of species at the FN-1 site, the new species associated with the younger sites, and the names of mapped lithostratigraphic units (SI). This figure shows results from other dating techniques: in red, amino acid racemization (Torres et al., 1997), black U-series/electron spin resonance for VM, FN3, ages for VM shows the maximum and minimum ages from five values, note an associated  $1\sigma$  error on all ESR ages (Duval et al., 2011, 12) and ESR dates for BL (Toro-Moyano et al., 2013). Note that carbonate accumulation in Venta Micena (Salar Valley) is lower than in Vélez Valley located near the Jurassic limestone Sierra de Orce (SI). Correlation between VM-2 (hominin site) and FN-3 is done using a key bed which consists of a dark fossiliferous silty clay that occurs below VM-2 and FN-3 sites. This key bed is named VM-1 in the Salar Valley (Anadón et al., 1987) and F-2 (also FN-2) in the Vélez Valley (Soria Rodríguez et al., 1987). (For interpretation of the references to colour in this figure legend, the reader is referred to the web version of this article.)

with the Olduvai subchron (1.93–1.77 Ma) and dated the lower part of the section to circa 2 Ma. This study assumed that the youngest preserved strata were deposited before Jaramillo, because the upper part of the studied stratigraphy was all of reverse polarity, producing minimum ages of 1.3 Ma for Venta Micena, 1.25 Ma for Barranco León, and 1.2 Ma for Fuente Nueva-3 (Scott et al., 2007) (Figs. 3, 4, S1). Oms et al., 2011 reviewed the available magnetostratigraphy for the Orce area, in this paper the lowermost lacustrine unit, associated with older fauna at the Galera C site (5 km downstream to the west of Orce), (Gibert et al., 2006a, 2006b), is correlated with our Fuentenueva lacustrine unit, which is stratigraphically and paleontologically younger, and well represented at the FN-1 site located 4 km upstream from Orce. The study

suggests that the 11.5 m normal episode identified near Orce, (Scott et al., 2007) should correspond to Gauss and that Olduvai was missing in the section due to sedimentary hiatuses. In 2015 two shallow boreholes at FN3 were used for additional paleomagnetic dating (Álvarez et al., 2015). Paleomagnetic directions were obtained from inclination values because the core was not oriented. Results are very discontinuous and show up to nine short normal episodes along the section. Although the upper normal event could fit with Cobb Mt. event, this discontinuous dataset does not agree with published results from Oms et al. (2000), or Scott et al. (2007) showing only reverse polarity for this stratigraphic interval in samples collected from nearby outcrops. This contradiction together with the low NRM intensities (in the order of  $10^{-6}$  A/m),

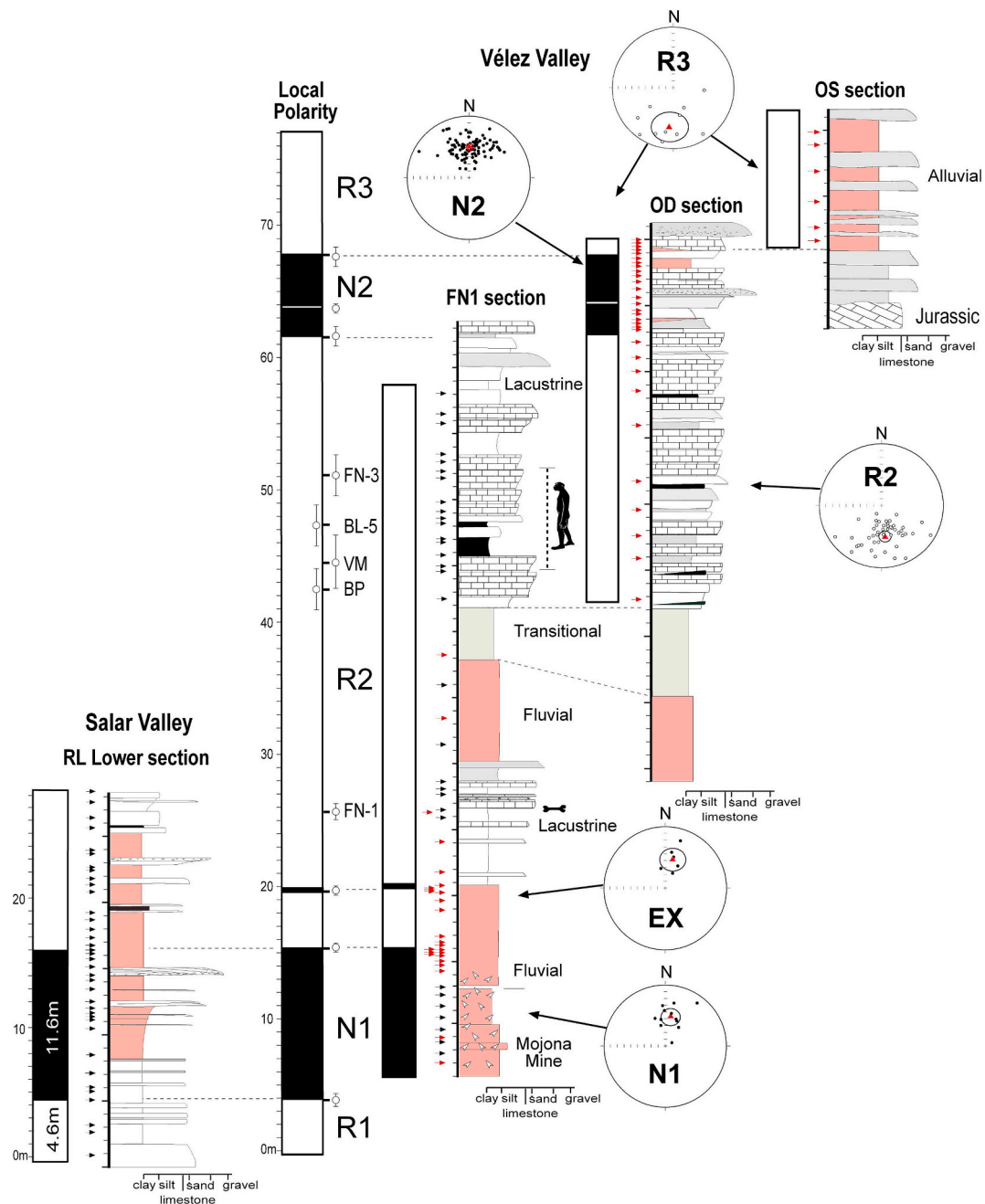


**Fig. 4.** Correlation of paleomagnetic results for results in lower Salar Valley (Scott et al., 2007) and the new results in the Velez Valley at FN-1, OD, and OS sections. The figure shows the local magnetic polarity sequence for the Velez Valley with four magnetic zones and the estimated stratigraphic position of different sites. The lower boundary of N1 and R1 zones only crops out in the deeper Salar Valley (Scott et al., 2007, S1). Red arrows are new samples, black arrows are published samples (Scott et al., 2007; Oms et al., 1996). Stereographic projections of paleomagnetic directions from the different magnetic zones are shown near the stratigraphy. N1 includes additional published specimens from Mojona Mine (Scott et al., 2007). EX shows mean directions for the excursion above zone N1. (For interpretation of the references to colour in this figure legend, the reader is referred to the web version of this article.)

suggest that the ChRM directions are probably secondary, and related to a non-removed viscous component associated with drilling operations, or to some diagenetic minerals. In addition, Álvarez et al. (2015) included a cosmogenic nuclide burial date from  $^{26}\text{Al}$  and  $^{10}\text{Be}$  in quartz grains. A single sample was collected at the level of the FN-3 site producing a minimum age of  $1.50 \pm 0.31$  Ma ( $1 \sigma$  uncertainty). The authors indicate that this age corresponds to a  $2 \sigma$  relative uncertainty range of 40%, so it should be considered with caution.

Three additional techniques were used to date the Orce sites. Amino acid racemization analysis on remains from gastropods produced an average age of  $983 \pm 58$  ka for Venta Micena (Torres et al., 1997). This

age was accepted by Torres et al. (1997) assuming an age of  $441 \pm 27$  ka for the site of Cullar Baza-1 obtained by the same technique. In 2007 a paleomagnetic study placed Cullar Baza-1 just above the Brunhes-Matuyama boundary ( $0.77$  Ma; Gibert et al., 2007a, 2007b) suggesting a considerable systematic error in the amino acid results. More recently, combined U-series/electron spin resonance (ESR) dating methods were applied to date the sites. Five mammal teeth were sampled from Venta Micena. The results gave ages between  $1.79 + 0.30/-0.23$  and  $0.57 + 0.08/-0.09$  Ma (standard errors at  $1 \sigma$ ) (Duval et al., 2011). In Barranco León and Fuente Nueva-3, nine teeth were analyzed, seven samples could not be dated, and the remaining two provided inconsistent ages of

1.19 ± 0.21 Ma and 0.52 + 0.09/−0.08 Ma for FN-3 (Daval et al., 2012). Finally, ESR dating was applied to optically bleached quartz grains from Barranco León (Toro-Moyano et al., 2013). Five sediment samples were analyzed from a 4.2 m stratigraphic interval that includes the BL-5 archaeological site (Gibert et al., 1998b) named level BL-D in Toro et al. 2013. The age estimates provided by Toro-Moyano et al. (2013) and stratigraphic positions with respect to the archaeological layer are: 1) sample BL-1, −1.5 m: 1.73 ± 0.17 Ma, 2) archaeological bed (sample BL-2): 1.46 ± 0.17 Ma, 3) samples BL-3 and BL-4 come from the same bed located, +0.9 m above the archaeological site, and produced ages of 1.88 ± 0.19 Ma and 1.23 ± 0.12 Ma, respectively, 4) sample BL-5 at +1.6 m above the archaeological site produced an age of 1.02 ± 0.09 Ma. Notice that the two ages from the same level differ by >0.65 Ma and that errors are 1  $\sigma$  or 68% confidence interval. The calculated age of the archaeological site is based on a weighted mean ESR age from three ESR samples obtaining a value of 1.43 ± 0.38 Ma at 1  $\sigma$  (or an error of ±0.76 Ma at 2  $\sigma$ ). Apart from the large error in this chronology, it is important to consider that according to these ESR ages, the lower boundary of the 4.2 m sampled interval (1.73 Ma) would be very close to the upper boundary of the Olduvai subchron (1.77 Ma), while the upper dated sample (1.02 Ma) would be included in the Jaramillo subchron (1.07–0.99 Ma). This stratigraphic interval is actually composed of tens of meters of reverse polarity (Fig. 3), suggesting that these boundaries are stratigraphically far apart, and therefore the ESR ages provided by Toro-Moyano et al. (2013) do not solve the chronology of the site. We conclude that prior chronologies for the Orce give a wide range of dates with large uncertainties that need to be refined to be useful in understanding the early hominin occupation of Europe.

## 2. Methods

### 2.1. Geological mapping of the Orce region

A new geological map for the Orce area (>50km<sup>2</sup>) was developed to support a chronostratigraphic framework. The map includes all paleontological sites ( $n = 15$ ) and the geographical distribution of lithostratigraphic units along the Salar and Vélez Valleys. We physically correlated (walked) the boundaries between units, paying particular attention to lithology, fossils, facies changes, sediment provenance, bed form, and potential discontinuities (Fig. 2, S2).

### 2.2. Lithostratigraphic correlations

Stratigraphic sections were measured at the paleontological sites of Venta Micena, Fuente Nueva 3, Fuente Nueva 1, Barranco del Paso, Barranco León and Orce D and Orce S. These sections were correlated using stratigraphic criteria as the boundaries between lithostratigraphic units. FN-1 site occurs in the FN lithostratigraphic unit, the remainder of the sites are included in the VM lithostratigraphic unit. To produce a correlation of beds inside this unit we use key marker beds, and polarity boundaries, together with topographical elevation and aerial videos following the stratigraphy, recorded with a drone (SI). All sites except Venta Micena, are located along the Vélez Valley where continuous outcrops exist simplifying the correlations between sites. To correlate Venta Micena (VM-2) with the nearby Fuente Nueva 3 section, located in the Salar Valley we use the key fossiliferous bed VM-1. VM-1 is a dark claystone rich in gastropods and small mammal fossils that occurs 2 m below VM-2 site which is the main vertebrate site in the area. VM-1 can be followed for >600 m from VM-3 quarry to VM-8 quarry (SI) and far south until the end of Barranco de los Zagales. This bed appears again 1.4 km south in Vélez Valley, 8.5 m below FN-3 site where it is named F2 or FN2 (Anadón et al., 1987; Soria Rodríguez et al., 1987). This layer occurs also above the FN-1 site and below BL-5. We estimated ±4 m of error in the vertical position of VM-2 bed and ± 3 m for FN-3.

The correlation between BP and BL-5 site located 600 m to the west, presents some difficulties due to the lateral facies change towards the

West. This change is visible between both sides of the Barranco del Paso (see Gibert et al., 1992). To make this correlation, we estimated the vertical distance by correlating the base of the palustrine carbonates, between these sections, providing an approximate distance of 5 m between BP and BL-5 (SI). We estimate ±3 m of error in the vertical position of the BP and BL sites (see SI). In respect to the correlation with the Mojona mine section, this can be considered as the same section as FN-1. This mine is located downstream about 300 m from FN1, below the valley surface at the RL lithostratigraphic unit, and overlaps with the FN1 section showing also the transition from normal to reverse polarity.

### 2.3. Digital elevation models

A Digital Elevation Model (DEM) was built for the studied region using ARCGIS 10.8 software with data from the National Geographic Institute of Spain (MDT02) with a 2 m resolution, revealing an area of previously unrecognized younger stratigraphy. Several topographic profiles were constructed based on this DEM to evaluate the elevations of stratigraphic sections (SI). A higher-resolution DEM and contour map was built in the area between Barranco León and the town of Orce where the stratigraphy preserves younger sediments. This detailed DEM included newly studied sections (OD and OS). It was constructed from an orthomosaic of georeferenced images obtained with a DJI Mavic 2 Pro drone flying at 100 m elevation, utilizing a Hasselblad camera at 20 Mp resolution. Images were processed with Agisoft Metashape software to reveal elevation differences between sections BL, OD, and OS, (Fig. S3).

### 2.4. Sampling strategy

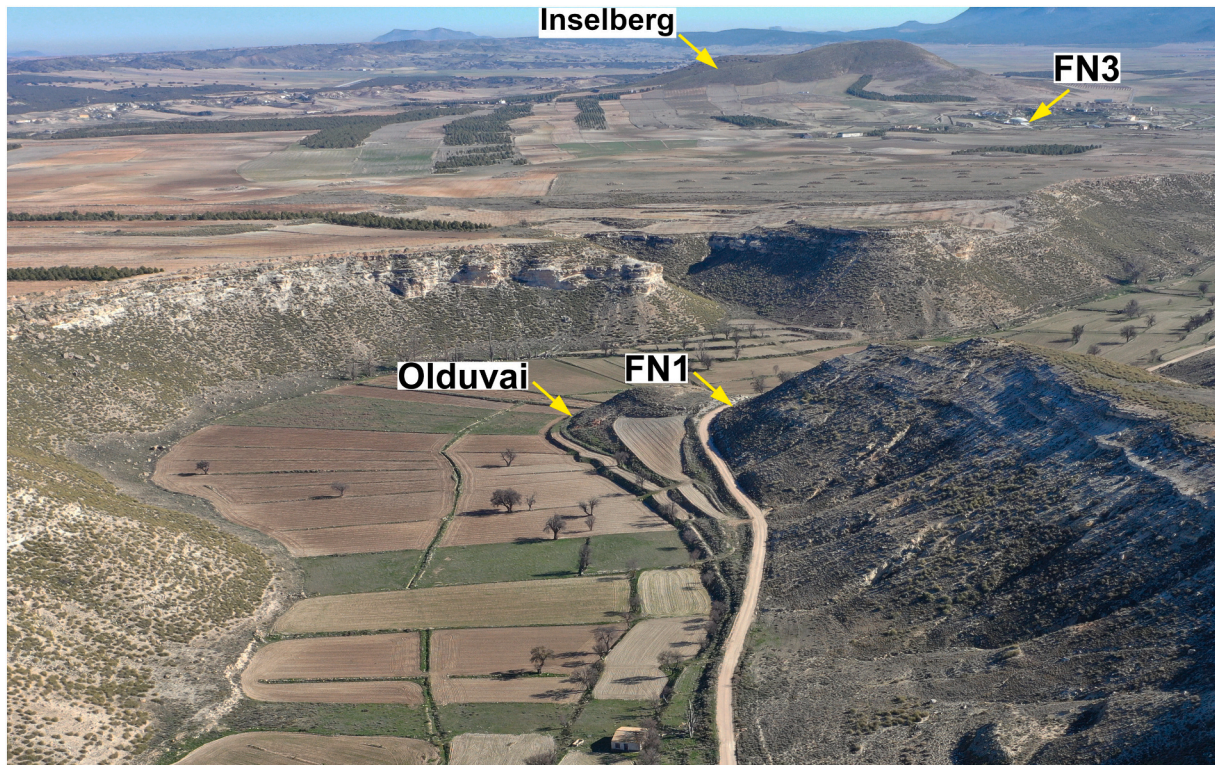
Initial paleomagnetic studies at Orce reported reverse polarity strata present at the sites, thus placing them below the Brunhes-Matuyama boundary and indicating an age older than 0.77 Ma (Oms et al., 1996, 2000). An expanded paleomagnetic study (Scott et al., 2007) reported a 11.5 m thick normal zone at the Salar Valley, interpreted as the Olduvai subchron (1.93–1.77 Ma). This normal zone was identified below the sites in the Vélez Valley at the Mojona mine (Scott et al., 2007) but the accurate position of the upper boundary was not determined. The absence of a second normal interval stratigraphically above the localities in reverse polarity constrained their paleomagnetic age to between 1.77 Ma (the top of the Olduvai) to 0.77 Ma (the base of the Brunhes-Matuyama boundary) (Muttoni et al., 2015). We expanded the magnetostratigraphy of the Vélez Valley in both lower and upper strata to more tightly constrain the age of the sites. We studied the lower 35 m of strata at the Fuente Nueva-1 section to locate the upper boundary of the Olduvai subchron and estimate the stratigraphic distance to the sites. In addition, we studied younger unsampled strata to identify additional paleomagnetic reversals that could help to constrain the age of the sites. Our detailed mapping of the region shows that these younger sediments are preserved at the Orce D (OD) and Orce South (OS) sections (Fig. 2, S2–4, field pictures 1 and 2).

### 2.5. Paleomagnetic methods

A total of 91 paleomagnetic samples were collected from the lower and uppermost strata in the Vélez Valley. The lower 35 m of the Fuente Nueva-1 section (27 samples), including two samples below the floor of the Vélez Valley at the nearby Mojona mine were sampled to locate the boundaries of the Olduvai subchron. The younger strata preserved at the nearby Orce D (OD) and Orce South (OS) sections were sampled to potentially locate the Jaramillo subchron. The OD section (39 samples; 29 m) as well as the OS section (6 samples; 8 m) overlying the OD section, extend to higher strata than previously investigated. Unaltered samples were obtained from artificial cave walls and small construction quarries or freshly exposed outcrops. Fine-grained lithologies were preferred (claystone, siltstone), although some limestone and fine sandstones were also collected. Most were block samples (500 to 1000



**Picture 1.** View of Barranco Leon site showing the location of the upper boundary of the Olduvai in the lower part of the Vélez Valley and the uppermost reverse paleomagnetic sample 5 m below an erosional surface.



**Picture 2.** Eastward view of the Vélez Valley showing the location of sampled FN1 section and the position of upper boundary of the Olduvai subchron (1.77 Ma). The figure shows the location of FN3 site near the Cerro de la Venta inselberg.

cm<sup>3</sup>) cut using manual tools, with one planar face oriented using a Brunton compass. The rest of the samples ( $n = 22$ ) were cylinders (2.5 cm diameter) collected with a battery-powered drilling tool. In the laboratory, each sample was sawed, sanded, and cleaned with compressed air, and at least three specimens (12 cm<sup>3</sup>) were obtained for the block samples. In the critical zones (polarity boundaries or newly defined magnetic zones), each sample station was re-sampled in a lateral equivalent position (same bed) to guarantee reproductivity. FN-1 section was sampled during the paleontological excavation of the FN-1 site led by J. Gibert and analyzed at the Berkeley Geochronology Center. Measurements of the OD and OS samples were performed at the Laboratory of Paleomagnetism in the Geosciences Barcelona Institute (CSIC/UB). The initial natural remanent magnetization (NRM) was measured on a superconducting rock magnetometer (2G Enterprises Ltd). After measuring the NRM, samples were analyzed using thermal demagnetization in 10 steps or more, starting at 100 °C and progressing stepwise in 50 °C increments in a non-inductive furnace (<10 nT) to remove unstable viscous remanent magnetizations and until the unblocking temperatures were reached and the samples were fully demagnetized. Magnetic susceptibility was measured with a KLY-2 susceptibility bridge after each demagnetization step, to monitor possible mineralogical changes during heating. Identification of ferromagnetic minerals was studied by means of Isothermal Remanent Magnetization (IRM) analysis and demagnetizing of the acquired magnetization. Paleomagnetic directions were calculated by means of principal component analysis (Kirschvink, 1980) using Remasof 3.0 software (AGICO Inc). To calculate the ChRM, we selected between 4 and 8 demagnetization steps between 250 and 600 °C, and a least-squares fit was made to the selected data points. The fit was not anchored to the origin of the Zijderveld plot since the ChRMs generally trended towards the origin and this option gave a better representation of the data quality (lower maximum angular deviation (MAD) values). The stratigraphic sequence of paleomagnetic directions is displayed as the angular difference ( $\Delta$ ) between a specimen direction and the expected Normal direction for this latitude [ $N = 000^\circ, 57^\circ$ ] (Hoffman, 1984). Plotting in this way specifically exposes the multiple-component nature of the measured vector data. The quality of the ChRM was estimated according to the delta ( $\Delta$ ) and MAD values. The best samples have at least two Class A specimens with  $\Delta$  values of 0°-30° for normal polarity, 150°-180° for reverse polarity, and MAD values <15°. Class B samples have specimens with increasing  $\Delta$  values between 30° and 150° and usually MAD values >15° which we interpret as ancient reverse polarity mixed with a persistent modern overprint that was only partially removed during demagnetization. Class C samples are poor-quality recorders that exhibit neither consistent directions nor trends. Polarity zonation was based on sequences of similar  $\Delta$  values of the higher temperature component line-fits and great-circle endpoints from class A specimens.

## 2.6. Micropaleontology

Rodent paleontological collections for all Orce sites stored at the Museu de l'Institut Català de Paleontologia Míguel Crusafont (IPS) in Sabadell, Spain were studied and compared with other European Early Pleistocene localities. In addition, a sample of 42 m1 photographs from TELRU *Allophaiomys lavocati* were studied and compared with the Orce *Allophaiomys* material. Measurements of the lower first molars were taken from these collections.

## 2.7. Age model

We use the obtained magnetostratigraphy to implement a Bayesian likelihood-based Markov Chain Monte Carlo technique for age-depth modeling of stratigraphic sequences, to build an accurate, high-resolution chronostratigraphic model. The Bayesian stratigraphic model is based on the Metropolis algorithm, wherein the likelihood of obtaining the observed data of a given model is calculated, followed by

adjustment of the model by perturbing parameters via a symmetric Gaussian proposal distribution, followed by acceptance of that proposal with a calculated probability. The model is evaluated every 2 cm of stratigraphic thickness. The age model is constrained in two ways: 1) it must be monotonically increasing in age with depth, and 2) the likelihood of the observed data corresponding to a proposed given model is calculated given the uncertainty of each data point and its absolute deviation from the proposed model age at the same depth (see Keller, 2018, Deino et al., 2019a, 2019b for details of the methodology).

## 3. Results

### 3.1. Geological mapping and stratigraphy

The new geological map for the Orce region supersedes previous maps (Soria Rodriguez et al., 1987; Oms et al., 2011; Toro-Moyano et al., 2013), allowing greater accuracy in the correlation of stratigraphic sections. Previous maps consider the lowermost deposits in the Vélez Valley as Pliocene (>2.6 Ma) and only distinguished three lithostratigraphic units (Vera et al., 1984). Previous maps show the basal lacustrine deposits at the confluence of Vélez and Salar Valleys and the lacustrine deposits at the locality of FN-1, located 4 km upstream, as the same units. However, Scott et al. (2007) reported that the lacustrine deposits at the confluence of the Salar and Vélez valleys show a normal zone in their upper levels that continue in the next 10 m of the overlapping alluvial unit. This normal zone is interpreted as the Olduvai subchron (Scott et al., 2007) and is positioned 10 m below the lacustrine deposits of FN-1 which are covered by younger Pleistocene alluvial deposits showing both units reversed polarity (Fig. S3). The distinction in the new map of two lacustrine units below the fossil sites has important stratigraphic implications since each lacustrine unit has a different faunal association that has previously led to confusion regarding the age of the lowermost deposits of the Vélez Valley (Oms et al., 2011). This new map shows three lacustrine episodes, the lowermost unit (Mo), has limited outcrops in the mapped area but crops out extensively downstream to the West along the Orce River below 925 masl (SI) and can be followed up to the town of Galera located 5 km West of Orce, where the fossil site Ga-C with small mammals older than FN-1 is exposed (Garcés et al., 1997). The upper two lacustrine units (FN and VM) show different associated vertebrate fauna separated by alluvial deposits. In total, five lithostratigraphic units are mapped, each reflecting the dominant sedimentary setting: lacustrine, fluvio-lacustrine or alluvial. These units are named within the sections where they are best exposed: Mo (Molino, lacustrine, UTM coord. 543451/4176387); RL (Rincón de la Losa, alluvial UTM coord. 547235/4177134); FN (Fuente Nueva-1, lacustrine UTM coord. 550249/4174860); TS (Torre del Salar, alluvial, UTM coord. 548969/4178346); and VM (Venta Micena, lacustrine, UTM coord. 552153/4176316), (Gibert et al., 2006a, 2006b). We notice that the thickness of the calcareous VM lithostratigraphic unit increases south towards the Sierra de Orce, which represents the main source of calcium carbonate (SI). It is also noticed that the thickness of the VM unit is more eroded in Salar Valley than in the Vélez Valley (SI).

All sites with human presence occur in the uppermost lacustrine unit (VM) that shows dominantly reverse polarity. Westward, near the town of Orce, these lacustrine deposits interfinger with alluvial fan deposits originating from the Sierra de Orce (Fig. 2 and S1–2).

### 3.2. Magnetostratigraphy

Our results expand the Orce magnetostratigraphy to a sequence with five magnetic zones (R1-N1-R2-N2-R3) in 80 m of strata, placing for the first time all paleontological/archaeological sites in the Vélez Valley between two normal zones (Figs. 3–5). R1, the lowest magnetozone, was described previously (Scott et al., 2007) at the oldest outcropping deposits that occur at the confluence of the Salar and Vélez Valleys and

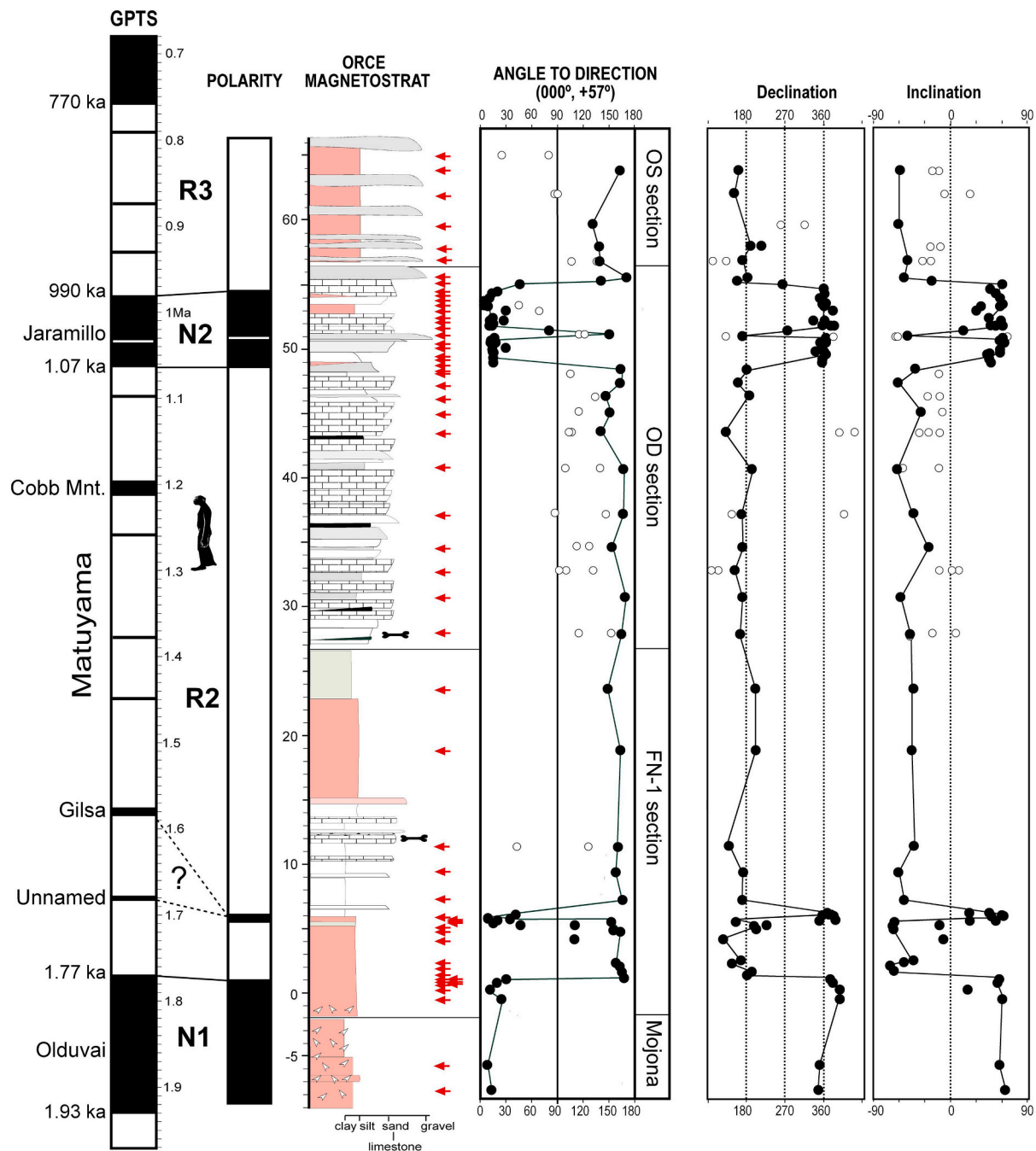


**Fig. 5.** Composite section for the Velez Valley with paleomagnetic directions (declination, inclination, and angle to the expected normal direction (Hoffman, 1984) for the lower FN-1, OD, and OS sections, showing the reverse polarity interval (R2), bearing human remains and tools, bounded by two normal zones (N1 and N2). The hominin figure shows the stratigraphic interval for hominin sites in R2. Results are correlated to the Geomagnetic polarity Time Scale (Ogg, 2020, Channell et al. 2020). The red arrows are new samples. Empty dots are specimen directions and black dots are mean values or selected specimen values for FN-1, OD, and OS sections (see table S1 for details on paleomagnetic directions). (For interpretation of the references to colour in this figure legend, the reader is referred to the web version of this article.)

further downstream along the Orce River, and is correlated with the early Matuyama Chron (Scott et al., 2007). N1 is 11.6 m thick, defined in the same section as R1 and correlated with the Olduvai Subchron (1.93–1.77 Ma) (Scott et al., 2007; Ogg, 2020; Channell et al., 2020), (Fig. 4). The upper boundary of N1 in the Vélez Valley is established in this study 10 m below the Fuente Nueva-1 paleontological site. Four meters above this boundary, a normal excursion has been identified and

correlated to an unnamed excursion located above the Olduvai or to Gilsa (Simon et al., 2018; Channell et al., 2020). We did this exercise to correlate this excursion with the following Gilsa excursion, and this does not affect substantially the proposed chronologies (SI). We did not correlate this excursion with younger events because this will generate abrupt changes in sedimentation rates (with an initial reduction and post-excursion acceleration), which are very difficult to justify in the

absence of important tectonic events not identified in the area.

R2 is the dominant magnetochron in the area and encompasses all archaeological sites. R2 was identified in previous studies in the Salar and Vélez Valleys (Scott et al., 2007; Toro-Moyano et al., 2013; Oms et al., 1996, 2000; Gibert et al., 2006a, 2006b), but its thickness was unknown because the boundaries were not located. Our results on the unsampled lower and upper strata demonstrate that R2 is ~47 m thick. N2 zone is represented by ~6 m of normal polarity strata above R2 in the upper OD section, is described here for the first time, and correlated to the Jaramillo Subchron (1.071–0.991 Ma) (Fig. 3–5, picture 3, SI). Within N2, a ~20 cm zone with intermediate directions is interpreted as an intra-Jaramillo excursion, identified previously in ocean cores, and in the nearby Cúllar section (Channell et al., 2020, Simon et al., 2018, Gibert et al., 2007a, 2007b). R3, also undescribed, is >6 m thick and includes reverse samples at the uppermost OD section and also at the overlying OS section.

Different alternative magnetozone correlations were considered but rejected. An older correlation would place the sites between the Gauss and Olduvai polarity episodes, indicating an age > 2 Ma for the archaeological sites; however, this is considered too old in light of the younger indications provided by the mammalian biostratigraphy and archaeology. Alternative interpretations of the sites being deposited between the Olduvai and Brunhes, or between the Jaramillo and Brunhes episodes, are excluded owing to the presence of reverse polarity above N2 (Figs. 3–5). A correlation of N2 with the Cobb Mt. event would make the sites a little older, but is more difficult to explain because it would generate very high sedimentation rates for N2 not compatible with sedimentation rates during N1 and R2. In addition, other dating techniques (burial dating, ERS biostratigraphy) suggest that the sites occur below the Jaramillo. The calculated primary and secondary (low temperature) directions are summarized in Supplementary Table 1.

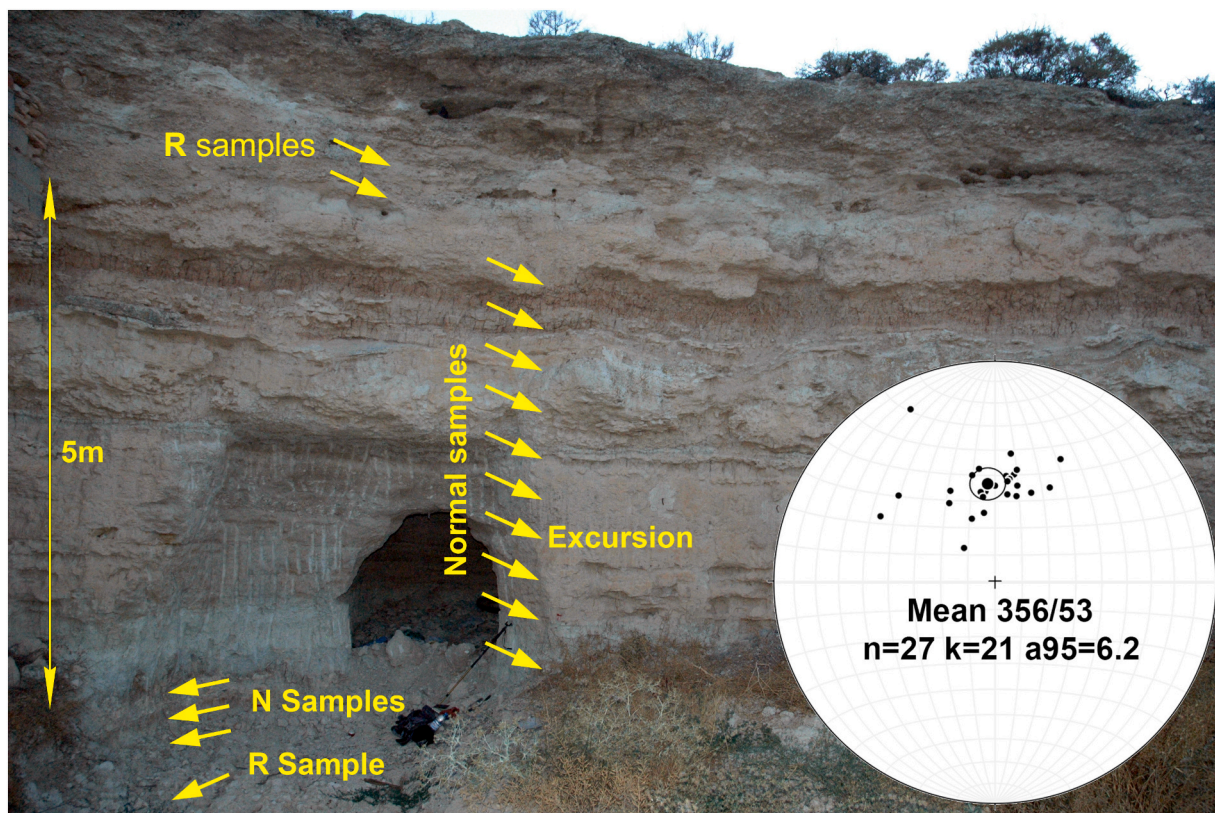
Representative demagnetization plots for each polarity zone are represented using Remasoft 3.0 software (Figs. 6 and S5).

### 3.3. Magnetic properties

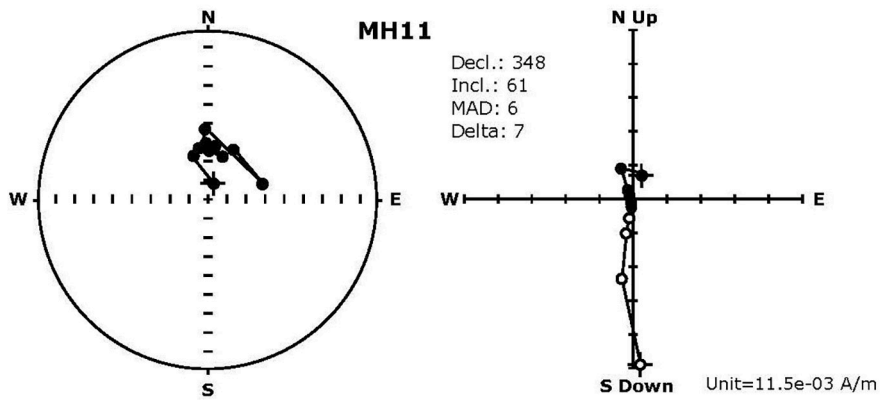
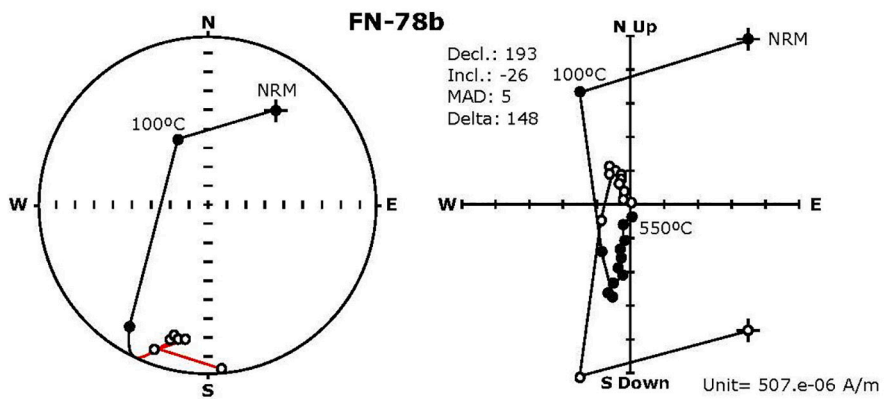
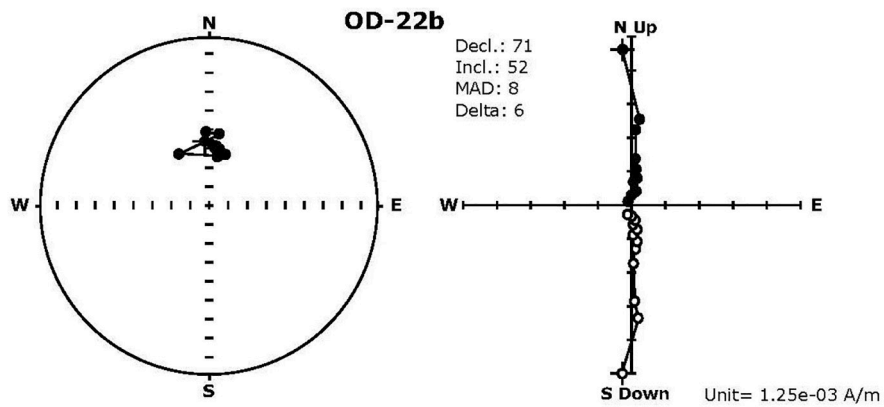
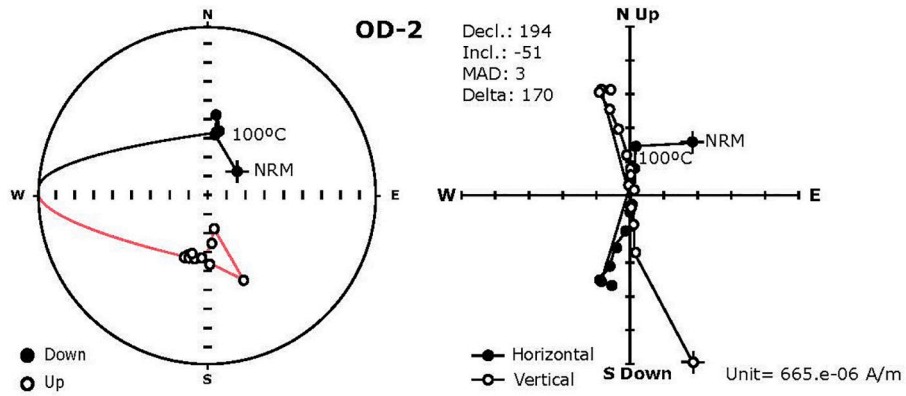
In general, samples revealed a primary characteristic direction, with specimens from most stations showing consistent normal or reverse directions (Class A). In ~25% of the samples, the secondary magnetization was not completely removed in all specimens, resulting in intermediate or inconsistent directions. Depending on the lithology, samples showed high to moderate magnetic susceptibility at room temperature. No major changes were recorded until the higher demagnetization steps (>550 °C), as shown by both susceptibility and remanence intensity. Most specimens have a two-component magnetization made up of a lower temperature or low coercivity component in the recent field direction and a higher temperature component in the normal or reverse direction. In the better recorders, a recent-field directed secondary component was effectively eliminated by heating to 200 °C. Overall the samples yielded unblocking temperatures of <600 °C, indicating magnetite as the main carrier of magnetization, although in some reddish specimens, the contribution of hematite appeared to be significant. This observation was confirmed by IRM analysis showing magnetite as a main contribution of magnetization in both normal and reverse samples (Figs. 7, 8).

### 3.4. Biostratigraphy

The paleontological information along the studied stratigraphic sequence is basic to correlate the local geomagnetic polarity sequence with the Geomagnetic Polarity Time Scale (Ogg, 2020, Channell et al., 2020). In the studied area, two groups of fossil vertebrates provide chronological information with different levels of accuracy. Large



**Picture 3.** Sample location for N2 zone along an excavated 8 m wall on the Western side of OD section equivalent to the Normal strata in picture 5 from the Eastern side. The figure shows the stereonet for ChRM directions of these samples showing a dominant Normal direction. Some samples in the uppermost and lowermost part of the outcrop show directions with delta values >30° which represent N + R components (class B). Reverse directions, also occur in the uppermost and lowermost positions of this outcrop not shown in the plot (see Table 1).



(caption on next page)

**Fig. 6.** Representative demagnetization stereoplots (left) and Zijderveld diagrams (right) for samples of Reverse 3 zone located in the highest stratigraphy from OD section (OD-2), normal zone N2 interpreted as Jaramillo from OD section (OD22b), sample from R2 zone at FN-1 section (FN-78b) and normal sample collected from the lowest part of FN-1 section from the N1 zone and correlated to Olduvai subchron (MH11). Figures drawn with Remasoft 3.0 software (AGICO). The plots show the stepwise demagnetization process. In the stereonet plots, open circles show negative inclinations and solid dots show positive inclinations. In the orthogonal plots, solid dots indicate declination values and empty circles inclination values. MAD is the maximum angle deviation. Delta is the angle to the expected normal direction of the primary magnetic direction. See SI Table 1 for details and for additional demagnetization plots.

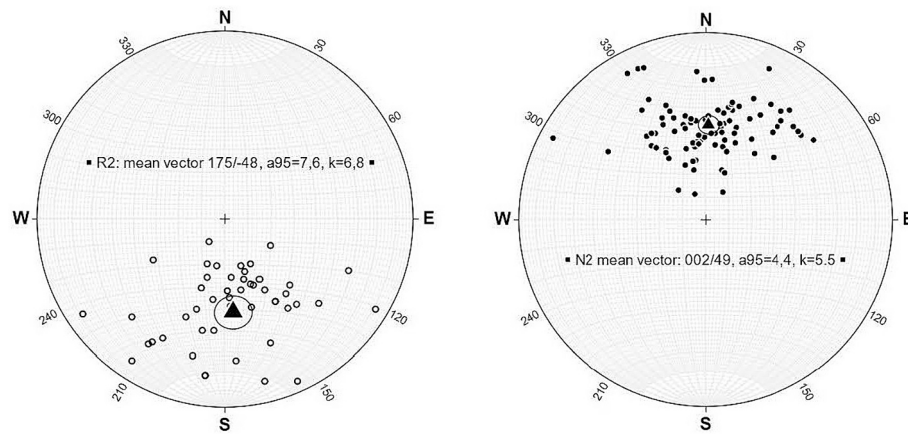


**Fig. 7.** stereographic projections for specimens from R2 and N2 zones including the mean vectors calculated with Stereonet 11 software. Empty circles show negative inclinations and solid dots show positive inclinations.

mammals are useful for defining large-scale mammal turnovers among different Eurasian sites, whereas small mammals, especially arvicolid rodents, can provide a more refined mammal chronology due to their high rates of evolution and species turnover. Large mammals recovered from sites in the Vélez Valley stratigraphy can be divided into two general faunal zones. The older is represented by the FN-1 site where, except for *Lynx* cf. *L. issiodorensis* and *Homo* sp., the large mammal species are also found at the site of Dmanisi, Georgia in a similar stratigraphic position above the Olduvai Subchron (Gabunia et al., 2000; Scott et al., 2007), (Table 1). The arvicolid rodents from Dmanisi have not been securely identified (Gabunia et al., 2000), but include only species with rhizodont (rooted) molars, as is the case at FN-1, suggesting a time before the immigration of the arhizodont *Allophaiomys*. This older mammal assemblage is typical of mammal zone MN17 (Table 1), supporting the placement of the terminal boundary of MN17 after the Olduvai Subchron (Opdyke et al., 1997). The second group of large mammals occurs at the stratigraphically younger sites of Barranco del Paso (BP), VM, BL-5 and FN-3, and includes the first appearance data for MQ1 mammal zone species including *Hippopotamus antiquus*, *Equus altidens* and *Homo*. The distribution of small mammals along the Vélez Valley permits us to further explore mammal replacement patterns. The BP quarry (~5 m below BL-5) produced the same species of large mammals ( $n = 7$ ) as VM, BL-5 and FN-3 but a different rodent association (Tables 1, 2). The large mammal fauna documents the first appearance datum (FAD) for *Hippopotamus antiquus* in the region, an African immigrant, associated with the rodents *Mimomys medasensis*, *Tibericola vandermeuleni*, *Allophaiomys* cf. *deucalion* and *Orcemys giberti* (Martin et al., 2017). BP was excavated in 1991 and 2001 but no conclusive evidence of human presence has been identified at the site. The rodent association at BP defines a separate faunal unit just below the sites with *Homo*. As a result, three superposed faunal units based on small mammals are proposed for the Early Pleistocene of Orce (Table 2). The location of the Jaramillo and the Brunhes-Matuyama boundaries at the nearby localities of Cúllar Baza and Huéscar-1 (Gibert et al., 2007a, 2007b, SI), shows sites with younger mammal association (Table 2).

### 3.5. The *Allophaiomys* from Orce sites

The Arvicolidae is a family of rodents including the voles, lemmings, and muskrats. Fossils of this group are often used for biostratigraphic dating of archaeological sites in North America and Europe because these rodents evolved rapidly and are often preserved in the fossil record in large numbers. Despite their abundance, a comprehensive arvicolid biostratigraphy is still not available for Europe. Because there is so much variation, and because there was such an explosive radiation of *Allophaiomys*-like voles subsequent to about 2.0 Ma, species boundaries are somewhat fuzzy, showing considerable overlap in measurements and ratios constructed from those measurements (Fig. 9). Older localities in Orce without *Allophaiomys*, such as Fuentenueva-1, are considered to have been deposited before the *Allophaiomys* immigration event into the Iberian Peninsula. *Mimomys* of indeterminate species is present at these localities. Higher in the Orce stratigraphy, molars potentially referable to *Allophaiomys* appear initially at Barranco del Paso (BP) and Barranco de los Conejos (BC), both at approximately the same stratigraphic level. In the next higher stratigraphic level, the *Allophaiomys* material from VM shows a more evolved morphology (more complex) and less arvicolid diversity. The *Allophaiomys* from VM was first assigned to *A. pliocaenicus* (Agustí, 1986; Agustí et al., 1987) and later to *A. ruffoi* (Agustí et al., 2010, Agustí and Madurell, 2003). The *Allophaiomys* from Barranco León 2-3 (BL-2-3) was also referred to *A. pliocaenicus* (Agustí, 1986, Agustí et al., 1987) but later the *Allophaiomys* from the archaeological site BL-5 (= BL-D), located 2 m above, was referred to *A. aff lavocati*. The latter species was also identified at Fuente Nueva-3 (FN-3) (Agustí and Madurell, 2003, Agustí et al., 2010). *A. lavocati* was named from the lowest unit in the Atapuerca cave system, TELRU (Trinchera Elefante, Lower Red Unit) (Laplana and Cuenca-Bescós, 2000). The identification of *A. lavocati* at BL-5 and FN-3 as well as from Atapuerca suggested an association between the appearance of *Homo* and this species in northern and southern Iberia at a similar time. However, *A. lavocati* from TELRU is associated with *Sus* sp., which is a biochronological marker in Europe (Martínez-Navarro et al., 2015), absent in the Orce region before 0.8 Ma. In addition, *A. lavocati* molars include a wider range of complexity than initially described (Laplana and Cuenca-Bescós, 2000), as subsequently more evolved and complex molars of *A. burgondiae* and

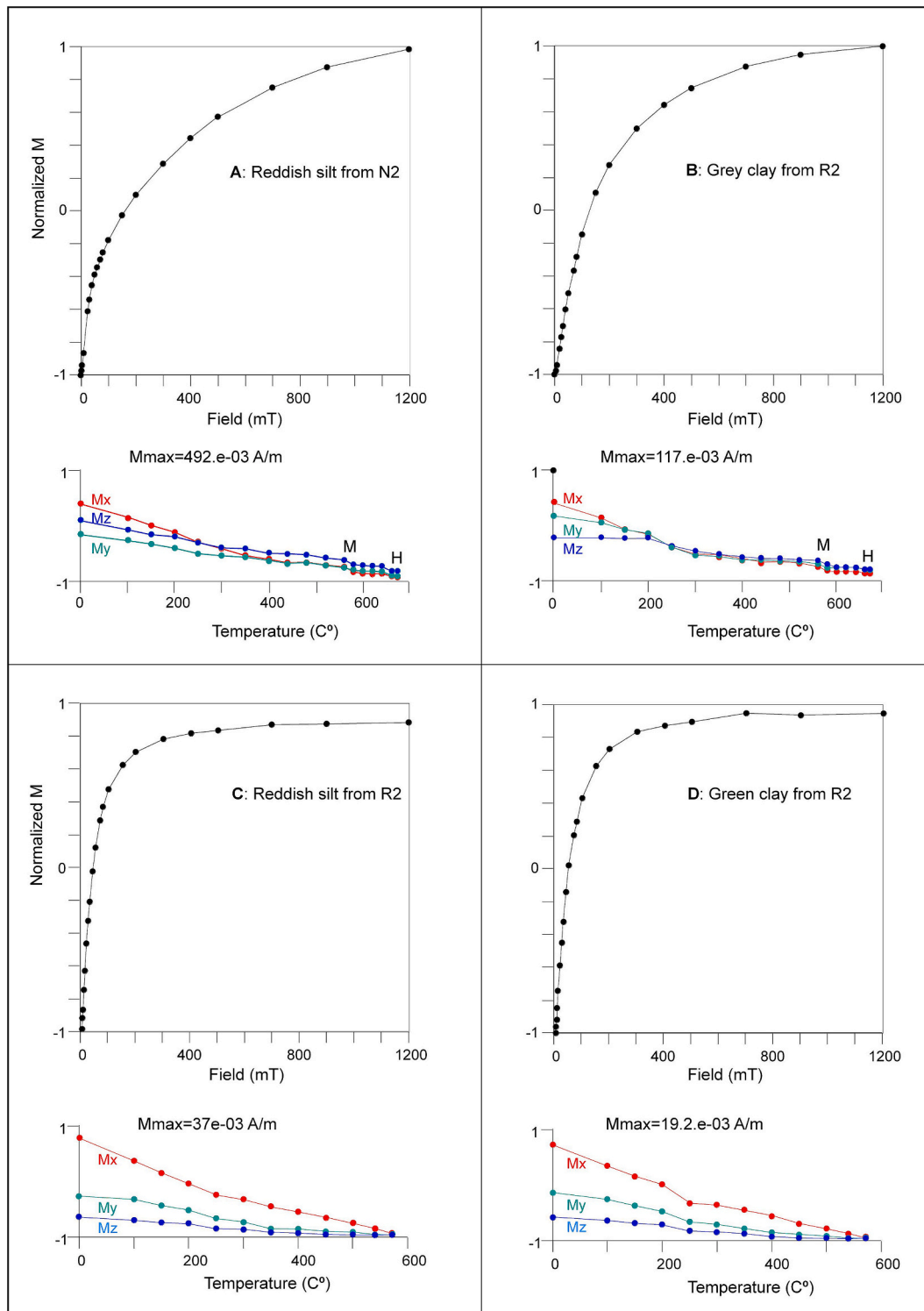


**Fig. 8.** IRM acquisition and 3-axis IRM demagnetization for different samples: reddish silt with normal polarity (A), grey clay with reverse polarity (B), reddish silt with reverse polarity (C) and green clay with reverse polarity (D). For each sample, it is shown: A) acquisition of IRM up to 1200 mT along the Z axis (normalized) above and B) thermal demagnetization of the 3-axis IRM. Notice that the samples below are characterized by the presence of a dominant magnetic phase that saturates at the field of  $\sim 300$  mT interpreted as magnetite (M). Samples above, but especially the reddish siltstone, show the presence of an additional higher coercivity phase interpreted as hematite (H). In those samples, saturation is not reached during IRM acquisition and demagnetization plots show decreasing magnetization after surpassing the Curie T of magnetite ( $\sim 575$  °C) and again after surpassing the Curie temperature of hematite ( $\sim 675$  °C). (For interpretation of the references to colour in this figure legend, the reader is referred to the web version of this article.)

**Table 1**

Large mammals for stratigraphically superposed sites in the Baza Basin that have been paleomagnetically dated. (FN1 = Fuente Nueva-1, BP=Barranco del Paso, VM = Venta Micena, BL-5 = Barranco Leon 5, FN3 = Fuente Nueva 3, HU-1 = Huéscar 1, CB1 = Cullar Baza 1, SZ = Solana del Zamborino). The table includes other reference Spanish sites outside the Baza Basin that have paleomagnetic data (TE 7–14 = Sima del Elefante levels 7–14, CV=Cueva Victoria, TD = Trinchera Dolina). Note that the site TE has more large mammal species in common with post-Jaramillo than with pre-Jaramillo sites and thus can be placed before or after Jaramillo. Data compiled from Mazo et al. (1985), Alberdi et al. (1989), Alberdi et al., 2001, García and Arsuaga (1999), van der Made (1999), Gibert et al., 2006a, 2002), van der Made and Mazo (2001), and Scott et al. (2007), Scott and Gibert, 2009, Gibert et al., 2016, Carbonell et al., 2008.

Magnetochrons (GPTS)	Olduvai	Matuyama						Jaramillo	Matuyama						Brunhes		
Approx. age (Ma)	1.95-1.77	1.6	1.3					1.07-0.99	0.98-0.79						0.75		
Lacustrine localities											Hu-1				CB1	SZ	
Karstic localities							TE7-14		TE7-14	CV			TD3-6a	TD6 b-7			
Stone tools																	
<i>Mamuthus trogontherii</i>																x	x
<i>Crocuta crocuta</i>																	x
<i>Elephas antiquus</i>																	
<i>Hippopotamus major</i>																	
<i>Ursus sp.</i>																	
<i>Theropithecus</i>																	
<i>Macaca sp.</i>																	
<i>Bison sp.</i>																	
<i>Sus sp.</i>																	
<i>Canis mosbachensis</i>																	
<i>Megaloceros sp.</i>																	
<i>Dama 'nestii' vallonnetensis</i>																	
<i>Panthera gombaszoegensis</i>																	
<i>Equus cf sussembornensis</i>																	
<i>Equus altidens</i>																	
<b>Homo</b>																	
<i>Eucladoceros giulii</i>																	
<i>Homotherium latidens / sp.</i>																	
<i>Pachycrocuta brevirostris</i>																	
<i>Megantereon sp.</i>																	
<i>Canis etruscus</i>																	
<i>Praeovibos sp.</i>																	
<i>Stephanorhinus etruscus</i>																	
<i>Ursus etruscus</i>																	
<i>Mamuthus meridionalis</i>																	
<i>Hippopotamus antiquus</i>																	
<i>Cervus perrieri</i>																	
<i>Gazella borbonica</i>																	
<i>Lynx issiodorensis</i>																	
<i>Equus stenonis</i>																	
<i>Pachycrocuta perrieri</i>																	



*A. nutiensis* were identified from TELRU (Cuenca-Bescós et al., 2013). The examination of a sample of 42 m1 molar photographs from TELRU *Allophaiomys lavocati* shows that the TELRU molars are, on average, consistently more advanced than those from VM, BL-5, and FN-3. For example, the majority of the m1s from VM, BL-5, and FN-3 do not exhibit a distinct T7 and LRA5 is rarely present and never filled with cement. A/L x C/W and B/W x C/W ratio plots are distinct for *A. lavocati* compared to the Orce samples. Consequently, we can conclude that the *Allophaiomys* from Orce sites is not *A. lavocati*, representing instead a more primitive *Allophaiomys* (Fig. 9, Table S3). In addition, the proposed different classification of VM *Allophaiomys* as *A. ruffoi*, suggests the VM site occurred before the arrival of humans. However, our study shows that there is little difference between the type populations of *A. pliocaenicus* and *A. ruffoi*, (Table S2), suggesting that *A. ruffoi* should probably be considered a junior synonym of *A. pliocaenicus* present at Barranco León and FN-3. The samples from VM fall within the morphospace delineated for the latter species (Fig. 9, Table S2). Although comparative data are not available for *Allophaiomys* m1s from BL-5 and FN-3, illustrations of m1s published (Agustí and Madurell, 2003) conform to those of *A. pliocaenicus* from the type locality (Betfia 2) and VM. Since there is no reliable way to distinguish *A. ruffoi* from *A. pliocaenicus*, and since the m1s from BL-5 and FN-3 are less advanced

than those of *A. lavocati* from TELRU, we can conclude that TELRU is younger than VM, BL-5 and FN-3. This conclusion is also supported by the large fauna association (Table 1) and previous observations (Scott et al., 2007). Agustí et al. (2022) recently added a new genus, *Manchenomys*, to the Orce arvicolid record. One species, *M. orcensis*, was recorded from FN-3. Although similar in morphology to *Allophaiomys*, *Manchenomys* apparently originated from a distinct small-sized *Mimomys* lineage and its presence at FN-3 does not alter the chronology presented here.

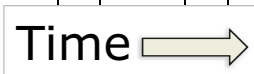
3.6. Bayesian age model and sites chronology

Having identified a detailed, extended magnetostratigraphy encompassing the fossil sites, we then estimated their age by stratigraphic interpolation. A Bayesian age-stratigraphic model was employed and formulated with the prior condition that strata monotonically decrease in age upward. The model considers all the available chronostratigraphic data, including estimated errors for the paleomagnetic chronozone boundaries and excursions (Simon et al., 2018) as well as potential errors in the stratigraphic position of boundaries and sites (Keller, 2018; Deino et al., 2019a, 2019b) (SI table-3). The final result of this algorithm is the posterior age distribution for each 2 cm of the

**Table 2**

Replacement chronology for Spanish arvicolid rodents over approximately the past 1 million years. Ma = millions of years ago, MPTS = magnetic polarity time scale. FN-1 = Fuente Nueva 1; OR-D = Orce D; BC = Barranco de los Conejos; BP = Barranco del Paso; OR-7 = Orce 7; VM = Venta Micena; BL-5 = Barranco León 5; FN-3 = Fuente Nueva 3; LRU = Lower Red Unit, Trincheras Elefante, Atapuerca; PL = Puerto Lobo; LQ = Loma Quemada; HU-1 = Huéscar 1; CN = Cueva Negra; D5 = Level D5, Cal Guardiola; TD3-8 A = Trincheras Dolina, Atapuerca Hills, levels D3-8 A; TD8B = Trincheras Dolina, Atapuerca Hills, level 8B; CB-1 = Cullar Baza 1; TD 10 = Trincheras Dolina, Atapuerca Hills, level 10. o = range-through record (species unrecorded but assumed to be present), x = present, cf. = compares favorably with, aff = has affinities with, ? = questionably present. Note that according to these fauna LRU can be placed before or after Jaramillo.

Magnetochrons (GPTS)	Olduvai		Matuyama						Jaramillo				Matuyama			Brunhes					
	1.95-1.77		1.6	1.4		1.3		1.07-0.99				0.98-0.79			0.78	0.75					
Localities	FN-1 OR-D		BC	BP	OR-7	VM	BL-5	BL-2	FN-3	LRU?	LRU?	PL	LQ	HU-1	CN	CV	D5	TD3-8a	TD8b	CB1	TD10
<i>Microtus agrestis</i>																					x
<i>Arvicola sapidus</i>																					cf
<i>Microtus arvalis</i>																					x
<i>Pliomys lenki</i>																					x
<i>Arvicola cantiana</i>																					cf
<i>Microtus atapuercensis</i>																			x		o
<i>Microtus sesae</i>																					x
<i>Microtus arvaldens</i>																					nr
<i>Iberomys huescarensis</i>														x	o	o	cf	cf			x
<i>Iberomys brecciansis</i>														cf	o	o	o	o	x	x	x
<i>Victoriamys chalinei</i>															x	x	x	x			x
<i>Microtus gregaloides /hintoni</i>														cf	x	o	o	x			x
<i>Ungaromys nanus</i>									x												x
<i>Pliomys episcopalpis</i>									x												x
<i>Arvicola jacobaeus</i>									x												x
<i>Allophaiomys lavocati</i>									x					cf	cf						x
<i>Mimomys savini</i>									o					x	x	x	x	o	x	x	
<i>Manchenomys orcensis</i>									x	x											x
<i>Allophaiomys pliocaenicus</i>									x	x											cf
<i>Allophaiomys deucalion</i>																					x
<i>Tibericola vandermeuleni</i>																					x
<i>Orcomys giberti</i>																					x
<i>Mimomys medasensis</i>																					x
<i>Mimomys sp.</i>																					x



section. Results of the model (Fig. 3) revealed a quasi-linear relationship of age to stratigraphic height, with a sediment accumulation rate of ~6.7 cm/ka (SI). Archaeological site age estimates and 95% confidence

interval generated by the Bayesian model are as follows: VM = 1.32 ± 0.07; BL-5 = 1.28 ± 0.07; and FN-3 = 1.23 ± 0.06 Ma. BP and FN-1 paleontological sites located below (-2 m and -18 m) strata with

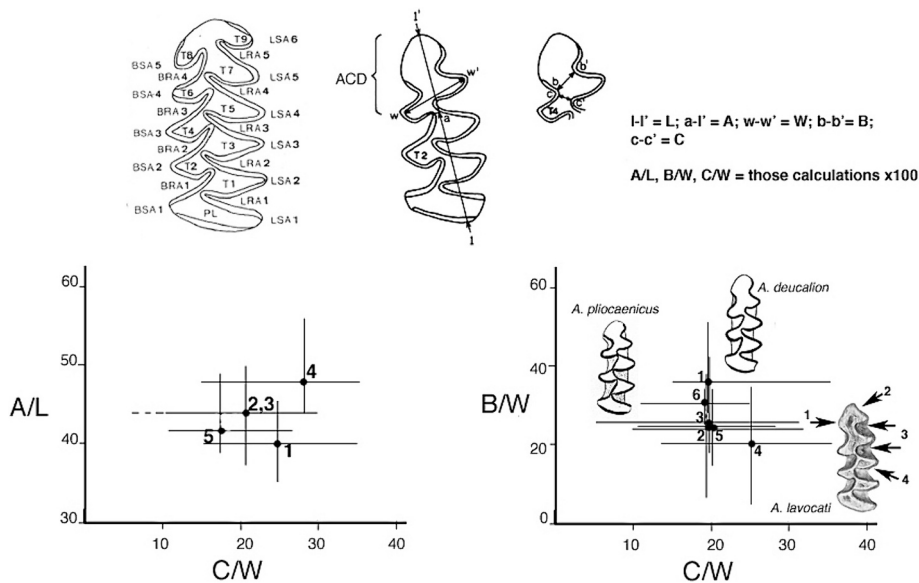


**Fig. 9.** First lower molar (m1) dental terminology (upper) and plots of A/L, C/W and B/W for m1s of *Allophaiomys deucalion*, *A. pliocaenicus*, *A. ruffoi*, and *A. lavocati* compared to *Allophaiomys* from Venta Micena. ACD = anteroconid, LRA = lingual reentrant angle, BRA = buccal reentrant angle, T = triangle, PL = posterior loop. 1 = *A. deucalion*, Villany 5; 2 = *A. pliocaenicus*, Betfia 2; 3 = *A. ruffoi*, Cava Sud; 4 = *A. lavocati*, TELRU; 5 = *A. pliocaenicus*, Venta Micena; 6 = *A. cf. deucalion*, Barranco del Paso. Black circles = grand means; lines = observed ranges. An average m1 morphotype is presented on the B/W x C/W graph for *A. pliocaenicus* (left, Fuente Nueva 3; from Agustí and Madurell, 2003), *A. deucalion* (top, Kryzhanovka 4; from Tesakov, 2004), *A. lavocati* (right, TELRU; No. 13, courtesy G. Cuenca-Bescós). Numbers on *A. lavocati* m1 correspond to the following: 1 = rudimentary T6; 2 = small but clearly developed T7, occasionally with cementum in LRA5; 3 = wide, horizontal “C-shaped” LRA3 and LRA4; 4 = positively differentiated enamel.

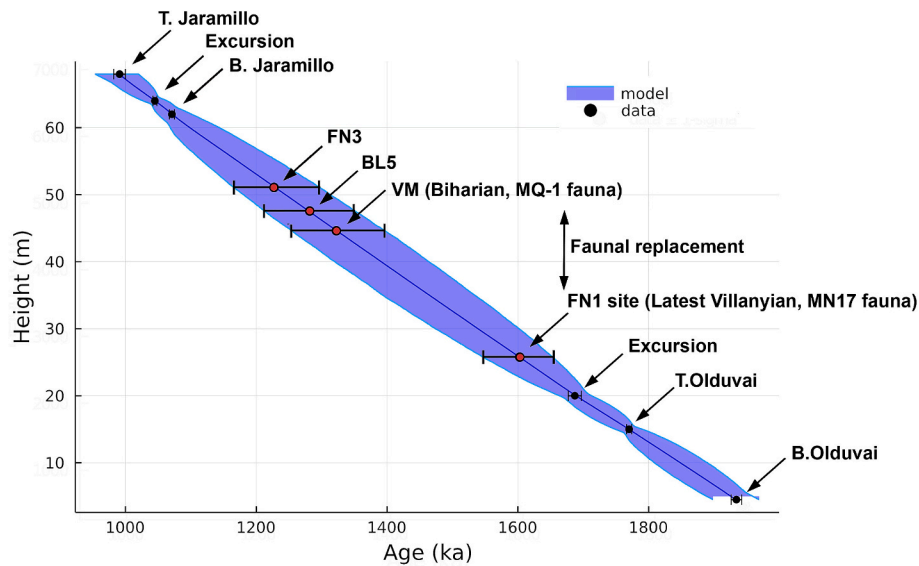


**Fig. 10.** Bayesian age-stratigraphic model for the Orce stratigraphy, based on six paleomagnetic reversals and excursions. The stratigraphic position for boundaries and sites comes from Fig. 4, see estimated errors in SI Table 3. The model identifies a quasi-linear depositional rate of 6.7 cm/ka. Interpolated model ages (red dots) for the sites ( $\pm$  95% confidence interval) are VM at  $1.32 \pm 0.07$  Ma, BL5 at  $1.28 \pm 0.07$  Ma, and FN3 at  $1.23 \pm 0.06$  Ma. The FN1 paleontological site (which lacks evidence of hominin occupation) is modeled at  $1.60 \pm 0.05$  Ma. (For interpretation of the references to colour in this figure legend, the reader is referred to the web version of this article.)

human presence and with different fauna, were dated at  $1.35 \pm 0.07$  and at  $1.60 \pm 0.05$  Ma respectively (Fig. 10). The alternative interpretation of the basal excursion as Gilsa (1.59 Ma, Ogg, 2020, Channel et al. 2020, Simon et al., 2018) instead of the unnamed excursion of Simon et al., 2018 (1.68 Ma) will make these chronologies only 15–20 ka younger and will produce a generally less linear sedimentation rate, (S7). The results of this model show similar ages for the sites. Finally, we produce a model ignoring the two identified excursions, and again this produces similar ages (SI table-3, SF7).

## 4. Discussion

### 4.1. Reliability of the normal zones

Persistent reversely magnetized sedimentary sequences on the Earth only occur before 0.77 Ma, following which normally magnetized sequences have occurred. Older sequences with normal polarity can be ambiguous (especially for flat-lying beds), either representing an ancient normally directed field or simply reflecting the normally directed modern field. Laboratory analysis, specifically progressive thermal demagnetization, is based on relaxation theory, such that increasing the thermal vibration relaxes magnetically fixed domains from domain populations that were fixed during progressively older and older times. Thus, the demagnetization reveals older magnetic directions at higher temperatures by removing the more recently formed directions. This process has an upper-temperature limit for each magnetic mineral (Curie temperature); for example, magnetite has a Curie temperature of 575 °C while Goethite which is a typical weathering (secondary) mineral has a Curie temperature of 120 °C. Secondary modern (normal) magnetisations were common in the NRM of our specimens but thermal demagnetization removed a large percentage of these younger vectors. Much higher percentages of modern normal vectors were removed from some weakly magnetized reverse specimens, such that the modern vectors could not be completely removed by laboratory demagnetisations. This appears to be the cause of intermediate directions in weak Class B specimens, with intermediate directions after thermal demagnetization. In horizontal strata such as these, the ancient Normal direction is subparallel to the modern weathering direction. We tested previous claims in Orce region of Normal zones interpreted as Olduvai,

showing that these zones corresponded to recent remagnetization (Scott et al., 2007; Gibert et al., 2006b). In this study, to resolve Normal polarity from ‘false Normal’ (modern field remagnetization), three tests were made: 1] Lithology Test - The polarity should be independent of lithology. Specifically, no correlation should exist between poor-quality recorders and apparent Normal polarity zones. 2] Stratigraphic Continuity Test (consistency test) - Magnetozone boundaries should be reproducible in nearby outcrops that can be stratigraphically correlated. Lateral continuity was tested at the OD area at distances of 100 and 200 m for N2 (SI) and 500 m (Mojona Mine) for N1. 3] Remanence/Polarity Similarity Test - This laboratory test demands that similar lithologic types have similar remanence features. Similarities in total vector spectra of coercivity and thermal demagnetization should be demonstrable regardless of polarity. Samples from N1 and N2 passed all three tests. Additional magnetic tests in these sedimentary rocks, including the fold test, were previously done in the N1 normal zone (Scott et al., 2007).

### 4.2. Sedimentary hiatuses

A topic of importance for calculating a chronology from magnetostratigraphic sections is any field observation of missing time which requires understanding the geologic context. Tectonics, climate and depositional settings control the pace and variability of sediment accumulation, hiatus and potential erosional events. The details for the Baza Basin depositional model were first presented to explain the extensive gypsum deposits that appear a few kilometers of Orce, towards the Basin’s depo-center. This model contains concentric lithofacies zones with decreasing salinity moving outward (Gibert et al., 2007b). The general conclusion is that the Baza Basin has rather continuous infilling, with >2.5 km of sediments accumulated between the latest Miocene and the middle Pleistocene (Haberland et al., 2017).

Orce occurs in the external facies belt of the Baza Basin, showing an alternation of freshwater palustrine carbonates and fluvial deposits displaying oxbows and meandering channels, suggestive of a very low gradient landscape affected by pedogenesis. In the most marginal areas, these deposits interfinger with marshes and alluvial sediments coming from the mountains that surround the basin.

We have not observed the ad-hoc paraconformities involving the loss

of hundreds of thousands of years of sediment (Oms et al., 2011) or unexpectedly sudden changes in accumulation rate in any of the magnetostratigraphic data published from the Baza Basin. Our current observations in both the Salar and Vélez Valleys support prior conclusions, that all hiatuses and discontinuities in this large, underfilled basin are minor (Scott et al., 2007). Small hiatuses exist in the short term, and are

identified in the normal and reverse zones within the numerous paleosols (calcsols) affecting fluvio-alluvial and palustrine deposits, but these consistently show immature features (thickness < 1 m, root traces, bioturbation, calcite nodules, pseudomicrocarst) indicating short duration for development (<1 ka) and rapid burial. The paleosols observed in the fluvial-alluvial and palustrine units do not show truncate B horizons

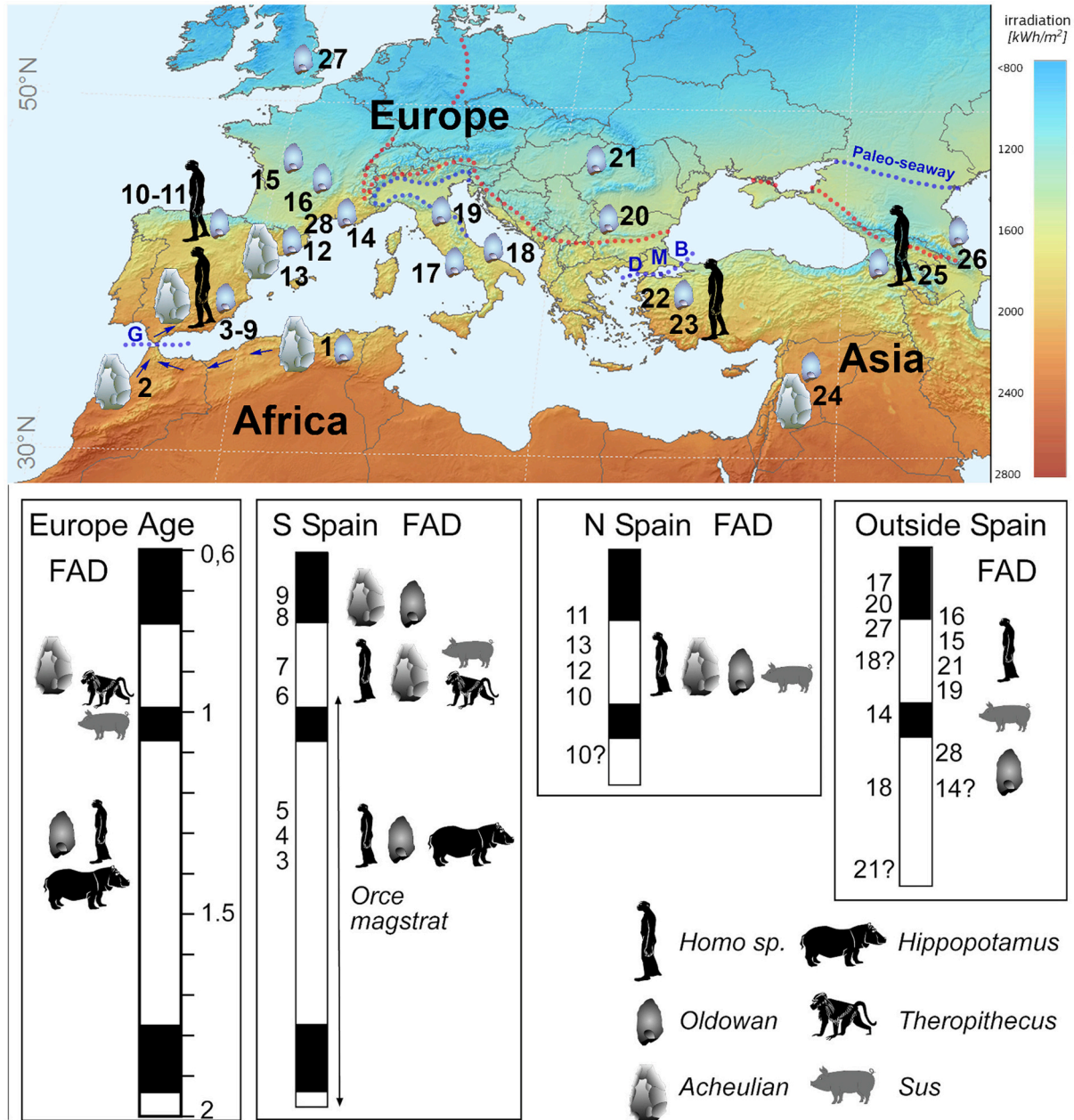


**Fig. 11.** Above: solar irradiation map of the Mediterranean region (Huld and Pinedo-Pasqua, 2014) showing key early human sites with hominin remains, Oldowan or Acheulian tools. G, D, B and M identify the Gibraltar, Dardanelles and Bosphorus straits and Marmara Sea that today separate Europe from Africa and Asia. Blue dotted lines are potential early Pleistocene marine biogeographical barriers, red dots indicate the limit of present daily freezing temperature during January (vividmaps 2016). Arrows show the proposed route for Oldowan and Acheulian hominines to reach Europe. Below: Updated magnetostratigraphy for Europe with associated sites and remains with the indication of first appearance datum (FAD) for African species (*Homo*, *Hippopotamus* and *Theropithecus*) and Asian species (*Sus*) in South, North Spain and outside Spain. *Hippopotamus* remains refer to initial occurrences at pre-Jaramillo hominin sites, since it is present in other post-Jaramillo sites. Notice that Early Pleistocene Acheulian sites are only reported in Spain and that the FAD of *Sus* is probably at the site of Le Vallonet where occurs associated with younger fauna than FN-3 but to normal polarity (Michel et al., 2017) 1 Ain Hanech, Ain Boucherit and El-Kherba, 2 Thomas Quarry, 3–5: VM, BL, FN3, 6: Cueva Victoria, 7: Cueva Negra, 8: Cullar Baza, 9: Solana del Zamborino, 10 Sima del Elefante, 11 Gran Dolina, 12 Vallparadis, 13 Barranc de la Boella, 14 Le Vallonet, 15 Pont-de-Lavaud, 16 Soleihac, 17 Isernia, 18 Pirro Nord, 19 Monte Poggiolo, 20 Kozarnica 21 Korolevo, 22 Gediz, 23 Kocabas, 24 Ubeidiya, 25 Dmanisi, 26 Mukhai-2, 27 Happisburg, 28 Bois-de-Riquet. For localities with more than one age, we refer to the oldest archaeological level. For localities with more than one age, we show with a question mark our non-preferred age. References for non-European sites: see Fig. 1, for other sites see Table 3. (For interpretation of the references to colour in this figure legend, the reader is referred to the web version of this article.)

and most of them can be described as cumulative paleosols that have slow but overall constant sedimentation rates where pedogenesis can modify the sediment as it is deposited (Kraus, 1999). Cumulative soils tend to preserve remains, such as artifacts or fossils (Holliday, 2004), that would be the case for most vertebrate sites at Orce that exhibit pedogenic features such of FN3 and VM. A few fluvial strata show minor erosional surfaces with limited lateral extent, which are typical basal bed features expected during stream migration and rising flood-stage scour. The deposition rate model for the Orce stratigraphy (Fig. S3), has frequent but short sedimentary interruptions resulting in a quasi-linear sediment accumulation rate in the long term.

#### 4.3. Implications for the oldest European hominin record

In northern Spain the level TE9 of Sima del Elefante (SE) hominin site has an estimated age of 1.2–1.1 Ma (Carbonell et al., 2008) based on two cosmogenic burial dates obtained below the Brunhes–Matuyama boundary and associated fauna. However, the Jaramillo subchron was not found and the formal statistical errors for the burial age estimates were quoted at only the 68% confidence interval indicating associated analytical uncertainties at 95% confidence interval of  $1.22 \pm 0.32$  Ma for TE9 and of  $1.13 \pm 0.36$  Ma for the stratigraphically older TE7 level located  $-4$  m below TE9. Considering the youngest and oldest cosmogenic burial ages the uncertainty in the age at 95% confidence interval of hominin level TE9 is 0.77 Ma to 1.54 Ma which allows placing this site also in a post-Jaramillo age, younger than 1 Ma (Muttoni et al., 2010, 2015; Muttoni and Kent, 2024). The small and large fauna from SE indicates a younger age than that found with *Homo* at Orce. The rodent *Allophaiomys lavocati* from SE is more advanced than the *Allophaiomys* recovered from the Orce sites (Toro-Moyano et al., 2013, Table 1). The large fauna includes mammals typically associated with younger biozones, such as opportunistic suids (pigs), (Table 1). Suids are considered good biostratigraphic and biochronological markers and have contributed greatly to understanding the chronology of East Africa sites (White and Harris, 1977; Cooke, 1978). Suids (*Sus strozii*) seems to disappear from the European fossil record before or during the Olduvai subchron (Martínez-Navarro et al., 2015), and reentered northern Spain during or after Jaramillo time, finding the first evidence in southern Spain in the early Pleistocene site of Cueva Negra (Walker et al., 2020), (Fig. 11). A recent study, identify suids at the site of Peyrolles in central France dated at 1.47 Ma (Iannucci, 2024) constraining the time without suids in Europe. This paper also proposes that the “Suid Gap hypothesis”, (Martínez-Navarro et al., 2015) could be a taphonomic artifact but considers an exception to the Orce sites due to the large number of fossils recovered.

Finally, a recent paper supplies cosmogenic nuclides ( $^{10}\text{Be}$ ,  $^{26}\text{Al}$ ) burial dates of  $1.42 \pm 0.28$  Ma ( $\pm 1\sigma$ ) for the oldest tool level of Korolevo site, (Ukraine). The large (20%) uncertainty range is the product of the high  $^{10}\text{Be}$  concentration in the samples, representing post-burial production. The authors better constrained the age by considering plausible estimates of post-burial production using the P-PINI method which yields a burial age of  $1.42 \pm 0.10$  Ma ( $\pm 1\sigma$ ), (Garba et al., 2024). As in the case of SE in Spain this chronology is supplied at 68% of confidence interval and should be taken with caution until additional dating is done (especially around the B/M boundary which could allow testing the error in the method). When initial uncertainties on the burial ages are supplied at 95% of confidence interval the age for Korolevo site is  $1.42 \pm 0.56$  Ma, which is compatible with the previously proposed post-Jaramillo age (Nawrocki et al., 2016).

For the first time in Europe three superposed stratigraphically sites are recognized between the Olduvai and Jaramillo subchrons, in the interval of  $\sim 1.32$ – $1.23$  Ma. According to our review, younger faunas, ambiguous magnetostratigraphic data or burial ages with large uncertainties characterize the remaining Early Pleistocene European sites (Muttoni et al., 2010, 2015, Muttoni and Kent, 2024). The Orce results can be considered the oldest solid evidence for humans in Europe

suggesting that humans entered southern Europe at  $>0.5$  Ma after they occupied Asia (Table 3).

#### 4.4. Asia occupied before Europe?

At present, Europe is separated from Africa by the Strait of Gibraltar and from Asia by the Marmara Sea and the so-called Turkish Straits (Dardanelles and Bosphorus). Two routes are possible to reach Spain from these ‘gates of Europe’: a long circum-Mediterranean route ( $>4000$  km), or a route from Africa via Gibraltar (at present 14 km). A third longer route across the Caucasus mountains and along the northern margin of the Black Sea would encounter a wide and cold paleo-seaway connecting the Caspian and the Black Sea (Krijgsman et al., 2019) and require a migration of  $>1500$  km in a region with present winter mean daily temperatures below  $0^\circ\text{C}$  (Vividmaps, 2016). Such a route seems unlikely for early hominin communities presumably lacking control of fire (Fig. 11). The connection between the Mediterranean and Black Seas has occurred discontinuously since Messinian times, associated with high global sea levels or Black Sea overflow into the Mediterranean. Though the chronology of connectivity is not well known (Krijgsman et al., 2019; Zubakov, 1988), this paleo-seaway could have presented an important barrier to westward early human and faunal expansion prior to the ice accumulation and associated global sea level fall initiated at 940 ka, during the Early-Middle Pleistocene Transition (Head and Gibbard, 2005). In addition, before 1 Ma the Po Valley in northern Italy was below sea level, also representing a limiting factor in early westward migration since an alternative route north of the Alps would be limited by temperature constraints (Muttoni et al., 2010, 2015, 2018), (Fig. 11).

When the archaeological record is examined in reference to this new European chronostratigraphic framework, we observe that the oldest Oldowan and later the oldest European Acheulian lithic assemblages are preserved at the early Pleistocene site of Orce (oldowan) and at Cueva Negra,  $37^\circ\text{N}$  latitude, (Scott and Gibert, 2009) and Barranc de la Boella ( $41^\circ\text{N}$ ) both in Iberia (Vallverdú et al., 2014), (Fig. 4). In this context, it is important to note that both technologies were present in northwestern Africa at  $36^\circ\text{N}$  latitude, in geographic proximity to Iberia, before appearing anywhere in Europe (Sahnouni et al., 2018; Scott and Gibert, 2009). A further cultural relationship between Spain and North Africa is indicated by features of the Oldowan techno-complex at Orce, such as subspheroidal morphologies, which are found also in the North African localities, but are absent at Dmanisi (Titton et al., 2020). We assert that the simplest explanation for the occurrence of the *Homo* toolmakers in southeastern Spain with technologies similar to those found in North Africa, before occurring anywhere else in Europe, is by the transit of the Strait of Gibraltar. Such a crossing would also help explain the presence of African hominids in SE Iberia predating the arrival of Asian suids to Orce (Martínez-Navarro et al., 2015, Iannucci, 2024), even though both share similar ecosystems. The available evidence shows that *H. erectus* indisputably crossed significant waterways during their southeastern migration to Flores Island in Indonesia, where archaeological remains show that *Homo* crossed the Wallace line, by navigating the paleo-Lombok Strait ( $>19$  km) before 1 Ma (Brumm et al., 2010). Recent research suggests that archaic *Homo* also used marine routes to reach the Philippines islands at 709 ka BP (Ingicco et al., 2018) and the island of Crete in the Mediterranean Sea at around 450 ka BP (Ferentinos et al., 2023). Thus, it is reasonable to postulate that hominins also crossed the paleo-strait of Gibraltar. Indeed, the presence of typically African fauna such as *Theropithecus* in southeast Spain in the Early Pleistocene site of Cueva Victoria or the first appearance data of Hippopotamus at Barranco del Paso, suggests that the Strait of Gibraltar acted as a filter-bridge sensu Simpson, (Simpson, 1940, Gibert et al., 1995; Gibert et al., 2006b; Ferrandez-Cañadell et al., 2014) rather than an impassable barrier. At present, the Gibraltar route requires crossing up to 14 km of seaway, although due to global eustatic cycles and high tectonic activity in this region, as evidenced by a sequence of raised Pleistocene shorelines as high as 210 m above present sea level (e.g., Rodríguez-Vidal

**Table 3**

updated chronology for early Pleistocene dated sites including statistical errors when available. The table includes other information such as the presence of tools/*homo* and the presence/absence of suids when fauna is available. Note that with 1.3 Ma the Orce sites appear in the group of sites older than 1 Ma with the most accurate dated.

Country/ region	Site	Age (Ma)	Uncertainty	Hominines	<i>Sus</i>	Tools	Technique	Deposit	References
<b>Western Asia</b>									
Georgia (Caucasus)	Dmanisi	1.77	—	X	—	Oldowan	40Ar/39Ar pmag	Basalt cavity infill	<a href="#">Gabunia et al., 2000</a>
Russia (Caucasus)	Muhkai II	>1.77?	—	—	—	Oldowan	pmag/fauna	Fluvial	<a href="#">Trifonov et al., 2019</a>
Turkey (Anatolia)	Kocabas	1.1–1.3	1 $\sigma$	X	No fauna	—	Pmag/ <sup>26</sup> Al/ <sup>10</sup> Be burial ages	Travertine	<a href="#">Lebatard et al., 2014</a>
Turkey (Anatolia)	Gediz	1170.2 $\pm$ 9.7 1246.6 $\pm$ 8.2	1 $\sigma$	—	No fauna	Oldowan n = 1	40Ar/39Ar pmag	Fluvial Terrace	<a href="#">Maddy et al., 2015</a>
<b>Europe</b>									
Ukraine	Korolevo level VII	0.77–0.99 1.42 $\pm$ 0.28	1 $\sigma$	—	No fauna	Oldowan	Pmag Burial dating	Fluvial Terrace	<a href="#">Nawrocki et al., 2016</a> <a href="#">Garba et al., 2024</a>
Bulgaria	Kozarnika Cave	<0.77	—	—	X	Oldowan	—	Karstic Fluvial/ estuarine deposits	<a href="#">Muttoni et al., 2017</a>
Great Britain	Happisburgh	0.77–0.99	—	—	—	Oldowan	Pmag	—	<a href="#">Parfitt et al., 2010</a>
France (south)	Le Vallonnet Complex 3	0.99–1.07	—	—	—	—	Pmag	—	—
	Complex 4	1.13 $\pm$ 0.15	2 $\sigma$	—	X	Oldowan	U-Pb on flowstone	Karstic	<a href="#">Michel et al., 2017</a>
France (east)	Complex 5	1.22 $\pm$ 0.09	2 $\sigma$	—	—	—	—	—	—
	Bois-de-Riquet	0.9–1	—	—	—	Oldowan	Biochronology	Basalt cavity infill	<a href="#">Lozano-Fernandez et al., 2019</a>
France (central)	Pont-de-Lavaud (Terrace D)	964 $\pm$ 100 1129 $\pm$ 160	1 $\sigma$	—	No fauna	Oldowan	ESR	Fluvial Terrace	<a href="#">Desprie et al., 2006</a>
France (central)	Soleihac	0.99–1.07	—	—	—	Oldowan	Pmag	Lacustrine	<a href="#">Thouveny and Bonifay, 1984</a>
Italy (north)	Monte poggiolo	0.85	—	—	No fauna	Oldowan	Pmag	Litoral	<a href="#">Muttoni et al., 2011</a>
Italy (central)	Pirro Nord	1.3–1.6 0.8	—	—	—	Oldowan	Pmag / ESR	Karstic	<a href="#">Pavia et al., 2012</a> <a href="#">Duval et al., 2024</a>
Italy (central)	Isernia	610 $\pm$ 10	2 $\sigma$	—	X	Oldowan	—	Lacustrine	<a href="#">Coltorti et al., 2005</a>
Spain (north)	Vallparadis	858 $\pm$ 87 0.77–0.99	1 $\sigma$	—	X	Oldowan	ESR/U-series Pmag	Alluvial	<a href="#">Duval et al., 2015;</a> <a href="#">Martínez et al., 2010</a>
Spain (north)	Barranc de Boella	0.77–0.99	—	—	X	Acheulian	Pmag	Alluvial	<a href="#">Vallverdú et al., 2014</a>
Spain (north)	Atapuerca, Gran Dolina, TD6	>0.77	—	X	X	Oldowan	Pmag Burial dating	Karstic	<a href="#">Parés and Pérez-González, 1999</a> <a href="#">Berger et al., 2008</a>
Spain (north)	Atapuerca, S. Elefante TE9	1.13 $\pm$ 0.18 0.77–0.99	1 $\sigma$	X	X	Oldowan	Pmag Burial dating	Karstic	<a href="#">Carbonell et al., 2008</a> <a href="#">Muttoni et al., 2010,</a> <a href="#">Muttoni and Kent, 2024</a>
Spain (South)0	Cueva Negra	0.77–0.99	—	X	X	Acheulian	Pmag	Karstic	<a href="#">Scott and Gibert, 2009</a>
Spain (South)	Cullar	0.75	—	—	X	Oldowan	Pmag	Lacustrine	<a href="#">Gibert et al., 2007a</a>
Spain (south)	Solana del Zamborino	0.75 0.4	—	—	X	Acheulian	Pmag	Lacustrine	<a href="#">Scott and Gibert, 2009</a> <a href="#">Álvarez-Posada et al., 2017</a>
Spain (South)	Cueva Victoria	0.77–0.99	—	X	—	—	Pmag, U/Th	Karstic	<a href="#">Gibert et al., 2016</a>
Spain (South)	Orce, Fuente Nueva-3	1.23 $\pm$ 0.06	2 $\sigma$	—	—	Oldowan	Pmag	Lacustrine	This study
Spain (South)	Orce, Barranco León	1.28 $\pm$ 0.07	2 $\sigma$	X	—	Oldowan	Pmag	Lacustrine	This study
Spain (South)	Orce, Venta Micena	1.32 $\pm$ 0.07	2 $\sigma$	X	—	?	Pmag	Lacustrine	This Study

et al., 2004); the paleo-Gibraltar strait was different and probably narrower in the past or even occasionally closed during late Messinian (6–5.3 Ma), favoring previous Afro-Iberian migrations (Gibert et al., 2003a; Gibert et al., 2016, 2013; Krijgsman et al., 2018).

## 5. Conclusions

The Orce region presents a unique European stratigraphic, paleontological, and hominin succession with >1 million years of the Early Pleistocene record. This study places three hominin sites within this record between the Olduvai and Jaramillo subchrons with dates of 1.32, 1.28, and 1.23 Ma. The Orce region recorded the first arrival of hominins in Europe ~1.3 Ma at the Venta Micena site, indicating that Europe was isolated from an Afro-Asiatic hominin world for >0.5 Ma, likely due to biogeographical barriers. Once hominins reached Iberia, they further dispersed into southern Europe. The archaeological record shows that a second wave of hominins with Acheulian lithic culture reached Europe (Iberia) after the Jaramillo, around 0.9 Ma. These chronologies suggest that the Strait of Gibraltar acted as a filter bridge for African species like hominins, *Theropithecus*, and hippos during the Early Pleistocene.

Supplementary data to this article can be found online at <https://doi.org/10.1016/j.earscirev.2024.104855>.

## CRedit authorship contribution statement

**Luis Gibert:** Conceptualization, Investigation, Methodology, Resources, Visualization, Writing – original draft. **Gary Scott:** Investigation, Methodology, Visualization, Writing – review & editing. **Alan Deino:** Formal analysis, Methodology, Visualization, Writing – review & editing. **Robert Martin:** Investigation, Methodology, Visualization, Writing – review & editing.

## Declaration of competing interest

The authors declare the following financial interests/personal relationships which may be considered as potential competing interests:

Luis Gibert reports financial support and travel were provided by Generalitat de Catalunya Ministry of Research and Universities. Luis Gibert reports financial support was provided by Spain Ministry of Science and Innovation. If there are other authors, they declare that they have no known competing financial interests or personal relationships that could have appeared to influence the work reported in this paper.

## Data availability

I have shared all data necessary to prepare this study in the main text and figures and as supplementary files

## Acknowledgments

We acknowledge Dr. Victoriano Pineda González for technical support with GIS and discussions in the field. Dr. Cuenca-Bescos kindly provided photos of *A. lavocati*. Dr. Bill Lukens solved some questions related to paleosols. Inst. Català de Paleontologia facilitates access to the arvicolid collections from Orce, projects of the Catalan Government (2017-SGR-824, 2021-SGR-349) and Spanish Government (CGL2016-79458-P, PID2020-118999GB-I00 [Spanish Ministry of Science and Innovation (MCIN)-510 State Research agency of Spain (AEI)/10.13039/501100011033] funded this research. Thanks to the Paleomagnetic Laboratory CcITUB - GEO3BCN CSIC and Berkeley Geochronology Center where the paleomagnetic analyses were conducted. Comments by Dr. Dan Palcu and two additional anonymous reviewers improved this manuscript. This article is dedicated to the memory of Dr. Josep Gibert Clois (1941-2007) who pioneered paleontological, paleoanthropological, and geological research at Orce, and promoted this study.

## References

- Aguirre, E., 2008. *Homo Hispanicus: la evolución del hombre en España 2008*. Editorial Espasa Calpe, S.a., p. 384.
- Agustí, J., 1986. Synthèse biostratigraphique du Plio-Pleistocene de Guadix-Baza (Province de Granada, sud-est de l'Espagne). *Geobios* 19, 505–510.
- Agustí, J., Madurell, J., 2003. Los arvicólidos (Muroidea, Rodentia, Mammalia) del Pleistoceno inferior de Barranco León y Fuente Nueva 3 (Orce, Granada). *Monografías de Arqueología*. Junta de Andalucía, Sevilla, pp. 137–145.
- Agustí, J., Moyà-Solà, S., 1987. Sobre la identidad del fragmento craneal atribuido a *Homo sp.* de Venta Micena (Orce, Granada). *Estud. Geol.* 43, 535–538.
- Agustí, J., Moyà-Solà, S., Pons-Moyà, J., 1987. La sucesión de mamíferos en el Pleistoceno inferior de Europa: proposición de una nueva escala biostratigráfica. *Paleont. i Evol esp* 1, 287–295.
- Agustí, J., Oms, O., Garcés, M., Parés, J.M., 1997. Calibration of the late Pliocene early Pleistocene transition in the continental beds of the Guadix Baza Basin (South Eastern Spain). *Quat. Int.* 40, 93–100.
- Agustí, J., Blain, H.-A., Furió, M., Marfá, R., Santos-Cubdeo, A., 2010. The early Pleistocene small vertebrate succession from the Orce region (Guadix-Baza Basin, SE Spain) and its bearing on the first human occupation of Europe. *Quat. Int.* 223–224, 162–169.
- Agustí, J., Piñero, P., Lozano-Fernández, I., Jiménez-Arenas, J.M., 2022. A new genus and species of arvicolid rodent (Mammalia) from the early Pleistocene of Spain. *Comp. Rendus Palevol* 21, 847–858.
- Alberdi, M.T., Alcalá, L., Azanza, B., Cerdeño, E., Mazo, A., Morales, J., Sesé, C., 1989. Consideraciones biostratigráficas sobre la fauna de Vertebrados fósiles de la cuenca de Guadix-Baza (Granada, España). In: Alberdi, M.T., Paolo, B. (Eds.), *Trabajos sobre el Neogeno-Cuaternario*. Museo Nacional de Ciencias Naturales, Madrid, pp. 347–355.
- Alberdi, M.T., Alonso, M.A., Azanza, B., Hoyos, M., Morales, J., 2001. Vertebrate taphonomy in circum-lake environments: three cases in the Guadix-Baza Basin (Granada, Spain). *Palaeogeogr. Palaeoclimatol. Palaeoecol.* 165, 1–26.
- Álvarez, C., Parés, J.M., Granger, D., Duval, M., Sala, R., Toro, I., 2015. New magnetostratigraphic and numerical age of the Fuente Nueva-3 site (Guadix-Baza basin, Spain). *Quat. Int.* 389, 224–234.
- Álvarez-Posada, C., Parés, J.M., Sala, R., Viseras, C., Pla-Pueyo, S., 2017. New magnetostratigraphic evidence for the age of Acheulian tools at the archaeo-paleontological site “Solana del Zamborino” (Guadix – Baza Basin, S Spain). *Sci. Rep.* 7, 13495.
- Anadón, P., Julià, R., de Deckker, P., Rosso, J.-C., Solulié-Marsche, I., 1987. Contribución a la paleolimnología del Pleistoceno inferior de la cuenca de Baza (sector Orce-Venta Micena). *Paleontol. i Evol. Mem. Espec.* 1, 35–72.
- Belmaker, M., Tchernov, E., Condemi, S., Bar-Yosef, O., 2002. New evidence of hominid presence in the lower Pleistocene of the Southern Levant. *J. Hum. Evol.* 43, 43–56.
- Berger, G.W., Pérez-González, A., Carbonell, E., Arsuaga, J.L., Bermúdez de Castro, J.-M., Ku, T.-L., 2008. Luminescence chronology of cave sediments at the Atapuerca paleoanthropological site, Spain. *J. Hum. Evol.* 55, 300–311.
- Borja, C., García Pacheco, J.M., García-Olivares, E., Scheuenstuhl, G., Lowenstein, J.M., 1997. Immunospecificity of albumin detected in 1.6 million-year-old fossils from Venta Micena in Orce, Granada, Spain. *Am. J. Phys. Anthropol.* 103, 433–441.
- Braun, D., Aldeias, V., Archer, W., Arrowsmith, R., Baraki, N., Campisano, C., Deino, A., DiMaggio, E., Dupont-Nivet, G., Redae, B., Feary, D., Garello, D., Kerfelew, Z., McPherron, S., Patterson, D., Reeves, J., Thompson, J., Reed, K., 2019. Earliest known Oldowan artifacts at >2.58 Ma from Ledi-Geraru, Ethiopia, highlight early technological diversity. *Proc. Natl. Acad. Sci.* 116 (24), 11712–11717.
- Brumm, A., Jensen, G.M., van den Bergh, G.D., Morwood, M.J., Kurniawan, I., Aziz, F., Storey, M., 2010. Hominins on Flores, Indonesia, by one million years ago. *Nature* 464, 748–752.
- Campillo, D., 1989. Study of the Orce man. In: Gibert, J., Campillo, D., Olivares, E., García (Eds.), *Los Restos Humanos de Orce y Cueva Victoria*. Institut Paleontologic Dr. M. Crusafont. Diputació de Barcelona, pp. 187–220.
- Campillo, D., Cuesta, M.M., García-Guixé, E., Devenat, L., Baxarias, J., 2006. An occipital crest in an infant cranium from the Roman necropolis of Francolí (Tarragona, Spain): Implications to the interpretation of the Orce skull. *Rev. Esp. Antropol. Fis.* 26, 93–103.
- Carbonell, E., Bermúdez de Castro, J.M., Pares, J., Pérez-González, A., Cuenca-Bescos, G., Ollé, A., Mosquera, M., Huguet, R., van der Made, J., Rosas, A., Sala, R., Vallverdú, J., García, N., Granger, D., Martinon-Torres, M., Rodríguez, X.P., Stock, G., Verges, J., Allue, E., Burjachs, F., Caceres, I., Canals, A., Benito, A., Díez, C., Lozano, C., Mateos, A., Navazo, M., Rodríguez, J., Rosell, J., Arsuaga, J.L., 2008. The first hominin of Europe. *Nature* 452, 465–469.
- Channell, J.E.T., Singer, B.S., Jicha, B.R., 2020. Timing of Quaternary geomagnetic reversals and excursions in volcanic and sedimentary archives. *Quat. Sci. Rev.* 228, 106–114.
- Coltorti, M., Cremaschi, M., Delitala, M.C., Esu, D., Fornaseri, M., McPherron, A., Nicoletti, M., Van Otterloo, R., Peretto, C., Sala, B., Schmidt, V., Sevink, J., 1982. Reversed magnetic polarity at an early Lower Palaeolithic site in Central Italy. *Nature* 300, 173–182.
- Coltorti, M., Feraud, G., Marzoli, A., Peretto, C., Ton-Thate, T., Voinchet, P., Bahain, J.-J., Minelli, A., Thun Hohenstein, U., 2005. New 40Ar/39Ar, stratigraphic and palaeoclimatic data on the Isernia La Pineta lower Palaeolithic site, Molise, Italy. *Quat. Int.* 131, 11–22.
- Cooke, H.S.B., 1978. Suid evolution and correlation of African hominid localities: an alternate taxonomy. *Science* 201, 460–463.
- Cuenca-Bescós, G., Rofes, J., López-García, J.M., Blain, H.-A., De Marfá, R.J., Rabal-Garcés, R., Sauqué, V., Arsuaga, J.L., Bermúdez de Castro, J.M., Carbonell, E., 2013.

- The small mammals of Sima del Elefante (Atapuerca, Spain) and the first entrance of Homo in western Europe. *Quat. Int.* 295, 28–35.
- Deino, A.L., Dommain, R., Keller, C.B., Potts, R., Behrensmeyer, A.K., Beverly, E.J., King, J., Heil, C.W., Stockhecke, M., Brown, E.T., Moerman, J., deMenocal, P., 2019a. Chronostratigraphic model of a high-resolution drill core record of the past million years from the Koora Basin, South Kenya Rift: Overcoming the difficulties of variable sedimentation rate and hiatuses. *Quat. Sci. Rev.* 215, 21–23.
- Deino, A., Sier, M., Garello, D.I., Keller, C.B., Kingston, J., Scott, J., Dupont-Nivet, G., Cohen, A.S., 2019b. Chronostratigraphy of the Baringo-Tugen-Barsemoi (HSPDP-BTB13-1A) Core:  $^{40}\text{Ar}/^{39}\text{Ar}$  dating, magnetostratigraphy, tephrostratigraphy, sequence stratigraphy and Bayesian age modeling. *Palaeogeog. Palaeoclimat. Palaeoecol.* 532. In: A high resolution, multi-proxy record of Pliocene hominin environments in the Kenya Rift Valley: Analysis of the Baringo-Tugen-Barsemoi (BTB) 109519.
- Desprée, J., Gageonnet, R., Voinchet, P., Bahain, J.J., Falguères, C., Varache, F., Courcimault, G., Dolo, J.M., 2006. Une occupation humaine au Pleistocène inférieur sur la bordure nord du Massif central. *Comp. Rendus. Palevol.* 5, 821–828.
- Diez-Martín, F., Sánchez, Yustos, P., Uribelarrea, D., Baquedano, E., Mark, D.F., Mabulla, A., Fraile, C., Duque, J., Díaz, I., Pérez-González, A., Yravedra, J., Egeand, C.P., Organista, E., Domínguez-Rodrigo, M., 2015. The Origin of the Acheulean: the 1.7 Million-Year-Old Site of FLK West, Olduvai Gorge (Tanzania). *Sci. Rep.* 5, 17839. <https://doi.org/10.1038/srep17839>.
- Duval, M., Bahain, J.J., Falguères, C., Garcia, J., Guilarte, V., Grün, R., Martínez, K., Moreno, D., Shao, Q., Voinchet, P., 2015. Revisiting the ESR chronology of the Early Pleistocene hominin occupation at Vallparadís (Barcelona, Spain). *Quat. Int.* 389, 213–223.
- Duval, M., Falguères, C., Bahain, J.-J., Grün, R., Shao, Q., Aubert, M., Hellstrom, J., Dolo, J.M., Agustí, J., Martínez-Navarro, B., Palmqvist, P., Toro-Moyano, I., 2011. The challenge of dating early Pleistocene fossil teeth by the combined US-ESR method: the case of Venta Micena palaeontological site (Orce, Spain). *J. Quat. Sci.* 26, 603–615.
- Duval, M., Falguères, C., Bahain, J.-J., Grün, R., Shao, Q., Aubert, M., Hellstrom, J., Dolo, J.M., Agustí, J., Martínez-Navarro, B., Palmqvist, P., Toro-Moyano, I., 2012. On the limits of using combined U-series/ESR method to date fossil teeth from two early Pleistocene archaeological sites of the Orce area (Guadix-Baza basin, Spain). *Quat. Res.* 77, 482–491.
- Duval, M., Arnold, L.J., Bahain, J.-J., Parés, J.M., Demuro, M., Falguères, C., Shao, Q., Voinchet, P., Arnaud, J., Berto, C., Berruti, G.L.F., Daffara, S., Sala, B., Arzarello, M., 2024. Dating the earliest evidence of human presence in western Europe: New results from Pirro Nord (Italy). *Quat. Geochronol.* 101519 <https://doi.org/10.1016/j.jqageo.2024.101519>.
- Ferentinos, G., Gkioni, M., Prevenios, M., Geraga, M., Papatheodorou, G., 2023. Archaic hominins maiden voyage in the Mediterranean Sea. *Quat. Int.* 646, 11–21.
- Ferrandez-Cañadell, C., Ribot, F., Gibert, L., 2014. New fossil teeth of *Theropithecus oswaldi* (Cercopithecoidea) from the early Pleistocene at Cueva Victoria (SE Spain). *J. Hum. Evol.* 74, 55–66.
- Ferring, R., Oms, O., Agustí, J., Berna, F., Nioradze, M., Shelia, T., Tappen, M., Vekua, A., Zhvania, D., Lordkipanidze, D., 2011. Earliest human occupations at Dmanisi (Georgian Caucasus) dated to 1.85–1.78 Ma. *Proc. Natl. Acad. Sci.* 108, 10432–10436.
- Gabunia, L., Vekua, A., Lordkipanidze, D., Swisher, C.C., Ferring, R., Justus, A., Nioradze, M., Tvalchrelidze, M., Anton, S.C., Bosinski, G., Jeoris, O., de Lumley, M. A., Majsuradze, G., Mouskhelishvili, A., 2000. Earliest Pleistocene hominin cranial remains from Dmanisi, Republic of Georgia: Taxonomy, geological setting, and age. *Science* 288, 1019–1025.
- Garba, R., Usyk, V., Ylä-Mella, L., et al., 2024. East-to-west human dispersal into Europe 1.4 million years ago. *Nature* 627, 805–810.
- Garcés, M., Agustí, J., Parés, J.M., 1997. Late Pliocene continental magnetostratigraphy in the Guadix-Baza basin (Betics, Spain). *Earth Planet. Sci. Lett.* 146, 677–687.
- García, N., Arsuaga, J.L., 1999. Carnivores from the Early Pleistocene hominid-bearing Trinchera Dolina 6 (Sierra de Atapuerca, Spain). *J. Hum. Evol.* 37, 415–430.
- Gibert, L., 2006. Análisis de facies y magnetostratigrafía de la Cuenca de Baza (Cordillera Bética). PhD Thesis. Universitat Politècnica de Catalunya.
- Gibert, L., 2008. Dr. Josep Gibert Clols, In memoriam. *Quat. Sci. Rev.* 27, 1091–1092.
- Gibert, J., Ferrández, C., 1989. Action anthropique sur les os à Venta Micena (Orce, Granada). In: Gibert, J., Campillo, D., García Olivares, E. (Eds.), *Los restos humanos de Orce y Cueva Victoria*. Institut de Paleontologia “Dr. M. Crusafont”, Sabadell, pp. 295–328.
- Gibert, J., Jiménez, C., 1991. Investigations into cut-marks on fossil bones of lower Pleistocene age from Venta Micena (Orce, Granada province, Spain). *Hum. Evol.* 4, 117–128.
- Gibert, J., Martínez-Navarro, B., 1992. Human presence and anthropic action in SE of the Iberian Peninsula during the lower Pleistocene. *Rev. Española Paleontol. Extra* 59–70.
- Gibert, J., Agustí, J., Moya, S., 1983. Fragmento craneal atribuido a Homo sp. de Venta Micena (Orce, Granada). In: *Paleontologia i Evolució, Int. Paleontologia Diputació de Barcelona. Special publication*, pp. 1–12.
- Gibert, J., Campillo, D., Ribot, F., Ferrández, C., Martínez-Navarro, B., Caporicci, R., 1989a. Comparative anatomical study of the cranial fragment from Venta Micena, (Orce, Spain) with fossil and extant mammals. *Hum. Evol.* 4, 283–305.
- Gibert, J., Ribot, F., Ferrández, C., Martínez, B., Caporicci, R., 1989b. Características diferenciales entre el fragmento de cráneo de Homo sp. de Venta Micena (Orce, Granada) y los équidos. *Estud. Geol.* 45, 121–138.
- Gibert, J., Arribas, A., Terán, J., Palomar, J., 1992. Contexto Geológico del Barranco del Paso. In: Gibert, J. (Ed.), *Presencia humana en el Pleistoceno inferior de Granada y Murcia*. Orce, Museo de Prehistoria y Paleontología Josep Gibert, pp. 203–217.
- Gibert, J., Ferrández, C., Martínez, B., Caporicci, R., Jiménez, C., 1992a. Roturas antrópicas en los huesos de Venta Micena y Olduvai. Estudio comparativo. In: Gibert, J. (Ed.), *Presencia humana en el Pleistoceno inferior de Granada y Murcia*. Museo de Prehistoria y Paleontología Josep Gibert, Orce, pp. 283–306.
- Gibert, J., Iglesias, A., Maíllo, A., Gibert, L., 1992b. Industrias líticas en el pleistoceno inferior de la región de Orce. In: Gibert, J. (Ed.), *Presencia humana en el Pleistoceno inferior de Granada y Murcia*. Museo de Prehistoria y Paleontología Josep Gibert, Orce, pp. 219–281.
- Gibert, J., Sánchez, F., Malgosa, A., Martínez, B., 1994. Découvertes de restes humains dans les gisements d’Orce (Granada, Espagne). *Comp. Rendus - Acad. Sci. Serie II: Sci. Terre Planet.* 319, 963–968.
- Gibert, J., Leakey, M., Ribot, F., Arribas, A., Martínez, B., Gibert, J., 1995. Presence of the genus *Theropithecus* in Cueva Victoria (Murcia, Spain). *J. Hum. Evol.* 28, 487–493.
- Gibert, J., Campillo, D., Arqués, J.M., García-Olivares, E., Borja, C., Lowenstein, J., 1998a. Hominid status of the Orce cranial fragment reasserted. *J. Hum. Evol.* 34, 203–217.
- Gibert, J., Gibert, L., Iglesias, A., Maestro, E., 1998b. Two ‘Oldowan’ assemblages in the Plio-Pleistocene deposits of the Orce region, southeast Spain. *Antiquity* 72, 17–25.
- Gibert, J., Gibert, L., Albaladejo, S., Ribot, F., Sánchez, F., Gibert, P., 1999. Molar tooth fragment BL-0: the oldest human remains found in the Plio-Pleistocene of Orce region (Granada province, Spain). *Hum. Evol.* 14, 3–19.
- Gibert, J., Gibert, L., Vicente, O., García, E., Ferrández, C., Iglesias, A., 2002. Excavación de urgencia en el yacimiento paleontológico Fuentesueva-1 (Orce, Granada). *Anuario Arqueológico de Andalucía. Activid. Urgencia* 1, 135–142.
- Gibert, J., Gibert, L., Iglesias, A., 2003a. The Gibraltar Strait: A Pleistocene Door of Europe? *Hum. Evol.* 18, 147–160.
- Gibert, J., Gibert, L., Vicente, O., 2003b. Memoria Preliminar de la actividad arqueológica en el yacimiento de Venta Micena, campaña 2003. Unpublished report. Inst. Català de Paleontologia, Sabadell, Spain.
- Gibert, J., Gibert, L., Ferrández-Cañadell, C., Iglesias, A., González, F., 2006a. Venta Micena, Barranco Leon-5 and Fuentesueva-3: Three archaeological sites in the Early Pleistocene deposits of Orce, south-east Spain. In: Ciochón, R.C., Fleagle, J.G. (Eds.), *The Human Evolution Source Book*. Pearson Prentice-Hall, pp. 327–335.
- Gibert, L., Scott, G.R., Ferrández-Cañadell, C., 2006b. Evaluation of the Olduvai subchron in the Orce ravine (SE Spain). Implications for Plio-Pleistocene mammal biostratigraphy and the age of Orce archaeological sites. *Quat. Sci. Rev.* 25, 507–525.
- Gibert, L., Scott, G., Martin, R., Gibert, J., 2007a. The early to Middle Pleistocene boundary in the Baza Basin (Spain). *Quat. Sci. Rev.* 26, 2067–2089.
- Gibert, L., Ortí, F., Rosell, L., 2007b. Plio-Pleistocene lacustrine evaporites of the Baza Basin (Betic Chain, SE Spain). *Sediment. Geol.* 200, 89–116.
- Gibert, L., Scott, G., Montoya, P., Ruiz-Sánchez, F.J., Morales, J., Luque, L., Abella, J., Lería, M., 2013. Evidence for an African-Iberian mammal dispersal during the pre-evaporitic Messinian. *Geology* 41, 691–694.
- Gibert, L., Scott, G.R., Scholz, D., Budsky, A., Ferrández, C., Ribot, F., Martin, R.A., Lería, M., 2016. Chronology for the Cueva Victoria fossil site (SE Spain): evidence for early Pleistocene Afro-Iberian dispersals. *J. Hum. Evol.* 90, 183–197.
- Haberland, C., Gibert, L., Jurado, M.J., Stiller, M., Baumann-Wilke, M., Scott, G., Mertz, D.F., 2017. Architecture and tectono-stratigraphic evolution of the intramontane Baza Basin (Betics, SE-Spain): Constraints from seismic imaging. *Tectonophysics* 709, 69–84.
- Harmand, S., et al., 2015. 3.3-million-year-old stone tools from Lomekwi 3, West Turkana, Kenya. *Nature* 521, 310–315.
- Head, M.J., Gibbard, P.L., 2005. Early-Middle Pleistocene transitions: an overview and recommendation for the defining boundary. Head, M.J. & Gibbard, P.L. (eds). *Early-Middle Pleistocene Transitions: the Land-Ocean Evidence*. *Geol. Soc. Lond. Spec. Publ.* 247, 1–18.
- Hoffman, K.A., 1984. A method for the display and analysis of transitional paleomagnetic data. *J. Geophys. Res.* 89, 6285–6292.
- Holliday, V.T., 2004. *Soils in Archaeological Research*. Oxford University Press, Oxford.
- Huld, T., Pinedo-Pasqua, I., 2014. Map of yearly sum of global irradiation. In: *Photovoltaic Geographical Information System (PVGIS) EU Science Hub* (europa.eu).
- Iannucci, A., 2024. *The Occurrence of Suids in the Post-Olduvai to Pre-Jarillo Pleistocene of Europe and Implications for Late Villafranchian Biochronology and Faunal Dynamics*. *Quaternary* 7 (1), 11. <https://doi.org/10.3390/quaternary7010011>.
- Ingicco, T., Bergh, G.D., Bahain, J.J., Chacon, M.G., Amano, N., Chacón M. G., Forestier, H., King, C., Manalo, K., Nomade, S., Pereira, A., Reyes, M.C., Sémah, A.M., Shao, Q., Voinchet, P., Falguères, C., Albers, P.C.H., Lising, M., Lyras, G., Yurnaldi, D., Rochette, P., de Vos Bautaista, A.J., 2018. Earliest known hominin activity in the Philippines by 709 thousand years ago. *Nature* 557, 233–237.
- Keller, C.B., 2018. Chron. j1: A Bayesian framework for integrated eruption age and age depth modelling.
- Kirschvink, J.L., 1980. The least-squares line and plane and the analysis of palaeomagnetic data. *Geophys. J. Int.* 62, 699–718.
- Kraus, M.J., 1999. Paleosols in clastic sedimentary rocks: their geologic applications. *Earth-Sci. Rev.* 47, 41–70.
- Krijgsman, W., Capella, W., Simon, D., Hilgen, F.J., Kouwenhoven, T.J., Meijer, P.T., Sierro, F.J., Tulpure, M.A., van den Berg, B.C.J., van der Schee, M., Flecker, R., 2018. The Gibraltar Corridor: Watergate of the Messinian Salinity Crisis. *Mar. Geol.* 403, 238–246.
- Krijgsman, W., Tesakov, A., Yanina, T., Lazarev, S., Danukalova, G., Van Baak, C.G.C., Agustí, J., Alçiçek, M.C., Aliyeva, E., Bista, D., Bruch, A., Büyükeremç, Y., Bukhsianidze, M., Flecker, R., Frolov, P., Hoyle, T.M., Jorissen, E.L., Kirschner, U., Koriche, S.A., Kroonenberg, S.B., Lordkipanidze, D., Oms, O., Rausch, L., Singarayer, J., van de Velde Stoica, M.S., Titov, V.V., Wesselingh, F.P., 2019.

- Quaternary time scales for the Pontocaspian domain: Interbasinal connectivity and faunal evolution. *Earth Sci. Rev.* 188, 1–40.
- Laplana, C., Cuenca-Bescós, G., 2000. Una nueva especie de *Microtus* (Allophaiomys) (Arvicolidae, Rodentia, Mammalia) en el Pleistoceno inferior de la Sierra de Atapuerca (Burgos, España). *Rev. Española Paleontol.* 15, 77–87.
- Larick, R., et al., 2001. Early Pleistocene <sup>40</sup>Ar/<sup>39</sup>Ar ages for Bapang Formation hominins, Central Java, Indonesia. *Proc. Natl. Acad. Sci.* 98, 4866–4871.
- Lebatard, A.E., Alçiçek, M.C., Rochette, P., Khatib, S., Violet, A., Bouibes, N., Bourles, D. L., Demory, F., Guipert, G., Mayda, S., Titov, V.V., Vidal, L., de Lumley, H., 2014. Dating the Homo erectus bearing travertine from Kocabas, (Denizli, Turkey) at least 1.1 Ma. *Earth Planet. Sci. Lett.* 390, 8–18.
- Lepre, C.J., Roche, H., Kent, D., Harmand, S., Quinn, R.L., Brugal, J.P., Texier, P.J., Lenoble, A., Feibel, C.S., 2011. An earlier origin for the Acheulian. *Nature* 477, 82–85.
- Lowenstein, J.M., Borja, C., Garcia-Olivares, E., 1999. Species-specific albinism in fossil bones from Orce, Granada, Spain. *Hum. Evol.* 14, 21–28.
- Lozano-Fernandez, I., Blain, H.-A., Agustí, J., Piñero P., Baskys, D. Ivorra J., Bourguignon, L., 2019. New clues about the late early Pleistocene peopling of western Europe: small vertebrates from the Bois-de-Riquet archeopaleontological site (Lezignan-La-Cebe, southern France). *Quat. Sci. Rev.* 219, 187–203.
- Luzón, C., Yravedra, J., Courtenay, L.L.A., Saarinen, J., Blain, H.-A., DeMiguel, D., Viranta-Kovanen, S., Azanza, B., Rodríguez-Alba, J.J., Herranz-Rodrigo, D., Serrano-Ramos, A., Solano, J.A., Oms, O., Agustí, J., Fortelius, M., Jiménez Arenas, J.M., 2021. Taphonomical and spatial analyses from the Early Pleistocene site of Venta Micena 4 (Orce, Guadix-Baza, Basin, southern Spain). *Sci. Rep.* 11, 13977 doi:10.1038/s41598-021-93261-1.
- Maddy, D., Schreve, D., Demir, T., Veldkamp, A., Wijbrans, J.R., van Gorp, W., van Hinsbergen, D.J.J., Dekkers, M.J., Schaife, R., Schoorl, J.M., Stemerink, C., van der Schriek, T., 2015. The earliest securely-dated hominin artefact in Anatolia? *Quat. Sci. Rev.* 109, 68–75.
- Martin, R.A., Tesakov, A., Agustí, J., Johnston, K., 2017. *Orcemys*, a new genus of arvicolid rodent from the Early Pleistocene of the Guadix-Baza Basin, southern Spain. *Comp. Rendus Palevol.* 17, 310–319.
- Martínez, K., García, J., Carbonell, C., Agustí, J., Bahain, J.J., Blain, H.A., Burjachs, F., Caceres, I., Duval, M., Falgueres, C., Gomez, M., Hugué, R., 2010. A new Lower Pleistocene site in Europe (Vallparadis, Barcelona, Spain). *Proc. Natl. Acad. Sci. USA* 107, 5762–5767.
- Martínez-Navarro, B., 2002. The skull of Orce: parietal bones or frontal bones? *J. Hum. Evol.* 42, 265–270.
- Martínez-Navarro, B., Madurell-Malapeira, J., Ros-Montoya, S., Espigares, M.P., Medin, T., Hortal, P., Palmqvist, P., 2015. The Epivillafranchian and the arrival of pigs into Europe. *Quat. Int.* 389, 131–138.
- Matsu'ura, S., Kondo, M., Danhara, T., Sakata, S., Iwano, H., Hirata, T., Kurniawan, L., Setiyabudi, E., Takeshita, Y., Hyodo, M., Kitaba, I., Sudo, M., Danhara, Y., Aziz, F., 2020. Age control of the first appearance datum for Javanese Homo erectus in the Sangiran area. *Science* 367, 210–214.
- Mazo, A.V., Sesé, C., Ruiz-Bustos, A., Peña, J.A., 1985. Geología y paleontología de los yacimientos Plio-Pleistocenos de Huéscar (Depresión de Guadix-Baza, Granada). *Estud. Geol.* 41, 467–493.
- Michel, V., Shen, C.C., Woodhead, J., Hu, H.M., Wu, C.C., Moullé, P.E., Khatib, S., Cauche, D., Moncel, M.H., Valensi, Chou, Y.H., Gallet, S., Echassoux, A., Orange, F., Lumley, H., 2017. New dating evidence of the early presence of hominins in Southern Europe. *Sci. Rep.* 7, 10074.
- Moyà-Solà, S., Köhler, M., 1997. The Orce skull: anatomy of a mistake. *J. Hum. Evol.* 33, 91–97.
- Muttoni, G., Kent, D.V., 2024. Hominin population bottleneck coincided with migration from Africa during the early Pleistocene ice age transition. *Proc. Natl. Acad. Sci.* 121 (13).
- Muttoni, G., Scardia, G., Kent, D.V., 2010. Human migration into Europe during the late early Pleistocene climate transition. *Palaeogeogr. Palaeoclimatol. Palaeoecol.* 296, 79–93.
- Muttoni, G., Scardia, G., Kent, D.V., Morsiani, E., Tremolada, F., Cremaschi, M., Peretto, C., 2011. First dated human occupation of Italy at ~0.85 Ma during the late Early Pleistocene climate transition. *Earth Planet. Sci. Lett.* 307, 241–252.
- Muttoni, G., Kent, D.V., Martin, R.A., 2015. Bottleneck at Jaramillo for human migration to Iberia and the rest of Europe? *J. Hum. Evol.* 80, 187–190.
- Muttoni, G., Sirakov, N., Guadelli, J.-L., Monesi, E., Kent, D.V., Scardia, G., Zerboni, A., Ferrara, E., 2017. An early Brunhes (<0.78 Ma) age for the Lower Paleolithic tool bearing Kozarnika cave sediments, Bulgaria. *Quat. Sci. Rev.* 178, 1–13.
- Muttoni, G., Scardia, Kent, D.V., 2018. Early hominins in Europe: the Galerian migration hypothesis. *Quat. Sci. Rev.* 180, 1–29.
- Nawrocki, J., Lanczont, M., Rosowiecka, O., Bogucki, A., 2016. Magnetostratigraphy of the loess-palaeosol key Palaeolithic section at Korolevo (Transcarpathia, W Ukraine). *Quat. Int.* 399, 72–85.
- Ogg, J.G., 2020. *Geomagnetic Polarity Time Scale. Geologic Time Scale. Chapter 5. Elsevier*, pp. 159–192. <https://doi.org/10.1016/B978-0-12-824360-2.00005-X>.
- Oms, O., Dinares Turell, J., Parés, J.M., 1996. Resultados paleomagnéticos iniciales de la sección Plio-Pleistocena de Venta Nueva (Cuenca de Guadix-Baza, Cordilleras Béticas). *Rev. Soc. Geol. Esp.* 9, 89–95.
- Oms, O., Parés, J.M., Martínez-Navarro, B., Agustí, J., Toro, I., Martínez-Fernández, G., Turq, A., 2000. Early human occupation of Western Europe: Paleomagnetic dates for two paleolithic sites in Spain. *Proc. Natl. Acad. Sci.* 97, 10666–10670.
- Oms, O., Anadon, P., Agustí, J., Julia, R., 2011. Geology and chronology of the continental Pleistocene archeological and paleontological sites of the Orce area (Baza basin, Spain). *Quat. Int.* 243, 33–43.
- Opdyke, N., Mein, P., Lindsay, L., Pérez-Gonzales, A., Moissenet, E., Norton, V.L., 1997. Continental deposits, magnetostratigraphy and vertebrate paleontology, late Neogene of Eastern Spain. *Palaeogeogr. Palaeoclimatol. Palaeoecol.* 133, 129–148.
- Pappu, S., Gunnell, Y., Akhilesh, K., Braucher, R., Taieb, M., Demory, F., Thouveny, T., 2011. Early Pleistocene Presence of Acheulian Hominins in South India. *Science* 331, 1596–1599.
- Parés, J.M., Pérez-González, A., 1999. Magnetostratigraphy and stratigraphy at Gran Dolina section, Atapuerca (Burgos, Spain). *J. Hum. Evol.* 37, 325–342.
- Parfitt, S.A., et al., 2010. Early Pleistocene human occupation at the edge of the boreal zone in Northwest Europe. *Nature* 466, 229–233.
- Pavia, M., Zunino, M., Coltorti, M., Angelone, C., Arzarello, M., Bagnus, C., Bellucci, L., Colombero, S., Marcolini, F., Peretto, C., Petronio, C., Petrucci, M., Pieruccini, P., Sardella, R., Tema, E., Villier, B., Pavia, G., 2012. Stratigraphical and palaeontological data from the early Pleistocene Pirro 10 site of Pirro Nord (Puglia, south eastern Italy). *Quat. Int.* 267, 40–55.
- Pope, G.G., 1983. Evidence on the age of the Asian Hominidae. *Proc. Natl. Acad. Sci.* 80, 4988–4992.
- Ribot, F., Gibert, L., Ferrández, C., Olivares, E.G., Sánchez, F., Lería, M., 2015. Two Deciduous Human Molars from the early Pleistocene Deposits of Barranco León (Orce, Spain). *Curr. Anthropol.* 56, 131–142.
- Rodríguez-Vidal, J., Caceres, L.M., Finlayson, J.C., Gracia, F.J., Martínez-Aguirre, A., 2004. Neotectonics and shoreline history of the region of Gibraltar, southern Iberia. *Quat. Sci. Rev.* 23, 2017–2029.
- Sahnouni, M., et al., 2018. 1.9-million-year-old artifacts and stone tool cut-marked bones from Ain Boucherit, Algeria. *Science* 362, 1297–1301.
- Sánchez, F., Gibert, J., Malgosa, A., et al., 1999. Insights into the evolution of child growth from lower Pleistocene homeri at Venta Micena (Orce, Granada province, Spain). *Hum. Evol.* 14, 63–82. <https://doi.org/10.1007/BF02436197>.
- Scott, G., Gibert, L., 2009. The oldest hand axes in Europe. *Nature* 461, 83–86.
- Scott, G., Gibert, L., Gibert, J., 2007. Magnetostratigraphy of the Orce region (Baza Basin), SE Spain: New chronologies for early Pleistocene faunas and hominid occupation sites. *Quat. Sci. Rev.* 26, 415–435.
- Simanjuntak, T., Semah, F., Gaillard, C., 2010. The palaeolithic in Indonesia: Nature and chronology. *Quat. Int.* 223–224, 418–421.
- Simon, Q., Bourlès, D.L., Thouveny, N., Horg, C.H., Valet, J.P., Bassinot, F., Choy, S., 2018. Cosmogenic signature of geomagnetic reversals and excursions from the Réunion event to the Matuyama-Brunhes transition (0.7–2.14 Ma interval). *Earth Planet. Sci. Lett.* 482, 510–524.
- Simpson, G.G., 1940. Mammals and land bridges. *J. Wash. Acad. Sci.* 30, 137–163.
- Soria Rodríguez, F.J., Lopez Garrido, A.C., Vera Torres, J.A., 1987. Mapa geológico sector Huéscar-Galera-Orce. Geología y Paleontología del Pleistoceno inferior de Venta Micena. *Paleontol. Evolució mem especial n° 1*.
- Tesakov, A., 2004. Biostratigraphy of middle Pliocene-Eopleistocene of eastern Europe. *Trans. Geol. Inst. Moscow* 554, 1–446.
- Thouveny, N., Bonifay, E., 1984. New chronological data on European Plio-Pleistocene faunas and hominid occupation sites. *Nature* 308, 355–358.
- Titton, S., Baskys, D., Bargalló, A., Serrano-Ramos, A., Vergés, J.M., Toro-Moyano, I., 2020. Subospheroids in the lithic assemblage of Barranco León (Spain): Recognizing the late Oldowan in Europe. *PLoS One* 15 (1), e0228290.
- Tobias, P.V., 1998. Some comments on the case for early Pleistocene Hominids in South-Eastern Spain. *Hum. Evol.* 13, 91–96.
- Toro-Moyano, I., Martínez-Navarro, B., Agustí, J., Souday, C., Bermúdez de Castro, J.M., Martín-Torres, M., Fajardo, B., Duval, M., Falgueres, C., Oms, O., 2013. The oldest human fossil in Europe, from Orce (Spain). *J. Hum. Evol.* 65, 1–9.
- Torres, T., Llamas, F.J., Canoria, L., García-Alonso, A., García-Cortes, A., Mansilla, H., 1997. Amino acid chronology of the lower Pleistocene deposits of Venta Micena (Orce, Granada, Andalusia, Spain). *Org. Geochem.* 26, 85–97.
- Torres, J.M., Borja, C., Gibert, L., Ribot, F., Olivares, E.G., 2022. Twentieth-Century Paleoproteromics: Lessons from Venta Micena Fossils. *Biology* 11, 1184. <https://doi.org/10.3390/biology11081184>.
- Trifonov, V.G., Tesakov, A.S., Simakova, A.N., Bachmanov, D.M., 2019. Environmental and geodynamic settings of the earliest hominin migration to the Arabian-Caucasus region: A review. *Quat. Int.* 534, 116–137.
- Vallverdú, J., Saladié, P., Rosas, A., Hugué, R., Cáceres, I., Mosquera, M., García-Tabernero, A., Estalrich, A., Lozano-Fernández, I., Pineda-Alcalá, A., Carrancho, Á., Villalafán, J.J., Bourlès, D., Braucher, R., Lebatard, A., Vilalta, J., Esteban-Nadal, M., Bennàsar, M.L., Bastir, M., López-Polín, L., Ollé, A., Vergés, J.M., Ros-Montoya, S., Martínez-Navarro, B., García, A., Martínell, J., Expósito, I., Burjachs, F., Agustí, J., Carbonell, E., 2014. Age and date for early arrival of the Acheulian in Europe (Barranc de la Boella, la Canonja, Spain). *PLoS One* 9 (7), Jul 30. e103634.
- van der Made, J., 1999. Ungulates from Atapuerca TD6. *J. Hum. Evol.* 37, 389–413.
- van der Made, J., Mazo, A.V., 2001. Spanish Pleistocene Proboscidean Diversity as a Function of Climate. The World of Elephants-International Congress, Consiglio Nazionale delle Ricerche Rome, pp. 214–218.
- Vera, J.A., Fernández, J., López Garrido, A.C., Rodríguez Fernández, J., 1984. Geología y estratigrafía de los materiales Plio-Pleistocenos del sector Orce-Venta Micena (Prov. Granada). *Paleontol. Evolució* 18, 3–11.
- Vividmaps, 2016. Map of average daily temperature for every month in Europe. <https://vividmaps.com/average-daily-temperature-for-every/>.
- Walker, M.J., Haber Uriarte, M., López Jiménez, A., López Martínez, M., Martín Lerma, I., van der Made, J., Duval, M., Grün, R., 2020. Cueva Negra del Estrecho del Río Quipar: a Dated late early Pleistocene Palaeolithic Site in Southeastern Spain. *J. Paleolithic Archaeol.* <https://doi.org/10.1007/s41982-020-00062-5>.
- White, T.D., Harris, J.M., 1977. Suid evolution and correlation of African hominid localities. *Science* 198, 13–21.

- Yravedra, J., Solano, J.A., Courtenay, L.A., Saarinen, J., Linares-Matás, G.J., Luzón, C., Serrano-Ramos, A., Herranz-Rodrigo, D., Cámara, J.M., Ruiz, A., Tittton, S., Rodríguez-Alba, J.J., Mielgo, C., Blain, H.-A., Agustí, J., Sánchez-Bandera, C., Montilla, E., Toro-Moyano, I., Fortelius, M., Oms, O., Barsky, D., Jiménez-Arenas, J.M., 2021. Use of meat resources in the Early Pleistocene assemblages from Fuente Nueva 3 (Orce, Granada, Spain). *Archaeol. Anthropol. Sci.* 13, 213.
- Yravedra, J., Solano, J.A., Herranz-Rodrigo, D., Linares-Matás, G., Saarinen, J., Rodríguez-Alba, J.J., Serrano-Ramos, A., Mielgo, C., Courtenay, L.A., Tittton, S., Blain, H.-A., Luzón, C., Cámara, J.M., Agustí, A., Sánchez-Bandera, C., Montilla, E., Toro-Moyano, I., Fortelius, M., Oms, O., Barsky, D., Jiménez-Arenas, J.M., 2022. Unravelling hominin activities in the zooarchaeological assemblage of Barranco León (Orce, Granada, Spain). *J. Paleolithic Archaeol.* 5, 6.
- Yravedra, J., Luzón, C., Solano, J.A., Linares-Matás, G.J., Estaca-Gómez, V., Rodríguez-Alba, J.J., Courtenay, L.A., Herranz-Rodrigo, D., Serrano-Ramos, A., Cámara, J., Saarinen, J., Sánchez-Bandera, C., Blain, H.A., Viranta, S., De Miguel, D., Azanza, B., Oms, O., Agustí, J., Fortelius, M., Jiménez-Arenas, J.M., 2023. To den or not to den. Contributions to the taphonomic history of the Early Pleistocene site of Venta Micena 4 (Orce, Guadix-Baza Basin). *Quat. Sci. Rev.* 308, 108031.
- Zhu, R.X., Potts, R., Pan, Y.X., Yao, H.T., Lü, L.Q., Zhao, X., Gao, X., Chen, L.W., Gao, F., Deng, C.L., 2008. Early evidence of the genus *Homo* in East Asia. *J. Hum. Evol.* 55, 1075–1085.
- Zhu, Z., Dennell, R., Huang, W., et al., 2018. Hominin occupation of the Chinese Loess Plateau since about 2.1 million years ago. *Nature* 559, 608–612.
- Zihlman, A.L., Lowenstein, J.M., 1996. A Spanish Olduvai? *Curr. Anthropol.* 37, 695–697.
- Zubakov, V.A., 1988. Climatostratigraphic scheme of the Black Sea Pleistocene and its correlation with the oxygen isotope scale and glacial events. *Quat. Res.* 29, 124.